Comparison of MODIS Binary and Fractional Snow Cover Mapping Techniques in the Himalayan Region, Nepal.

by

Preeti Tuladhar

A RESEARCH PAPER

submitted to

THE DEPARTMENT OF GEOSCIENCES
OREGON STATE UNIVERSITY

in partial fulfillment of the
requirements for the
degree of

MASTER OF SCIENCE

GEOGRAPHY PROGRAM

June 2006

Directed by
Dr. Anne W. Nolin

Comparison of MODIS Binary and Fractional Snow Cover Mapping Techniques in the Himalayan Region, Nepal.

ABSTRACT

Satellite remote sensing is an effective tool for mapping snow covered area. However, complex terrain and heterogeneous land cover, due to vegetation and patchy snow cover, present challenges to snow cover mapping. This research compares two techniques for mapping snow covered area: binary and enhanced fractional snow cover mapping techniques. Both are implemented using data from the Moderate Resolution Imaging Spectroradiometer (MODIS). Two study regions with the differing amounts of vegetation are used in this investigation: Everest National Park, and Annapurna Conservation Area, both located in Nepal. The MODIS binary product maps a pixel as snow if roughly 50% or more is snow. It also incorporates a vegetation correction and cloud mask. The MODIS Snow Covered Area and Grain Size/Albedo (MODSCAG) product gives the fraction of snow cover in each MODIS pixel, but does not incorporate a vegetation correction or cloud mask. Landsat ETM+ images are used to assess the accuracy of each product. Results show that MODSCAG provides a more accurate mapping of snow cover in a heterogeneous landscape, where snow cover is patchy. However, the MODIS binary product is more accurate for mapping snow cover in heavily forested regions. Accuracy of the two techniques varied with elevation, MODSCAG being more accurate as elevation increased. The results presented in this paper will help improve understanding of snow cover mapping techniques and aid future planning of water resources in climatologically sensitive regions.

1 INTRODUCTION

1.1 Importance of Snow Cover and Mapping Complexities

In high latitude and high elevation regions, melt water derived from the snow pack represents the greatest contribution to stream discharge (Barnett, 2005). Although remoteness and geographic complexities makes them difficult to study, mountainous regions are very important, as these environments are sensitive to climate change, land use change and alterations to the hydrological cycle. For example, devastating flooding can result from various environmental changes including seasonal temperature variability causing additional snow melt (Barnett, 2005). Conversely, less than average snow melt can lead to water deficits. For countries that rely on snow melt to sustain agriculture and infrastructure, scarcity of water will have catastrophic impact.

Moreover, land use change, such as deforestation, plays a pivotal role in influencing the hydrological cycle by intensifying the surface runoff and increasing the instances of flooding and landslides downstream (Ichii et al., 2003). Previous studies done by Jordan (1994) showed that extensive deforestation, particularly on steep hillsides of Nepal, has led to widespread increase in geomorphic activity. Deforestation has been going on in mountainous countries such as Nepal since the middle of the 20th century and the rate of deforestation has been increasing since 1960s (Stevens, 2003). Vegetation influences the accumulation and ablation of a seasonal snow cover and many studies have demonstrated the effect of vegetation on snow cover (Golding and Swanson 1986, Hedstrom and Pomeroy 1998, Storck et al 2003). Data from various field experiments have demonstrated that forest canopies alter the snow pack energy balance (Hardy et al., 1998). Murray and Buttle (2003) found that snow accumulation in the clear-cut exceeded that of the forest, and the melt was significantly larger in the clear-cut than in the forested areas. Therefore, the dynamics of snow accumulation and ablation in the forested vs. non-forested regions have huge effect on the water resources.

To predict extreme events, accurate hydrological modeling and precise prediction of stream flow is needed. For stream flow prediction, snow covered area (SCA) has long been recognized as an important hydrological variable (Hall and Martinec, 1985). Satellite-derived measurements of SCA have been used effectively as an input to snowmelt runoff models such as SRM models (Rango and Martinec, 1979). Therefore, estimating snow cover accurately is needed to evaluate the runoff from snow melt and, hence, predict its impact to the region. However, satellite snow cover mapping in the forested regions have been complicated due to the presence of canopy cover over snow. Nevertheless, remotely sensed SCA provides the only information on the spatial and temporal distributions of snow and subsequent snow melt where field data are difficult to obtain or do not exist. Naturally, for countries like Nepal with its rugged terrain and remoteness and where snow melt is the largest contributors to rivers and ground water (Chalise et al., 2003), the only effective method of periodic snow cover mapping and stream flow prediction is by satellite remote sensing. Hence, it is important to measure and quantify the extent of snow cover over diverse landscape as accurately as possible, especially in the regions that depend on snow melt for water resources.

1.2 Physical Basis of Snow Cover Mapping from Space

Snow is one of the brightest objects in nature in the optical and near-infrared range (~0.41– 1.4 μm), and is dark in the medium-infrared (~1.5 – 2.5 μm). Spectral reflectivity of snow is dependent on snow parameters, such as grain size and shape, impurity content, near-surface liquid water content, depth and surface roughness, and on solar illumination (Warren, 1982). In the visible wavelengths ice is highly transparent, making the albedo of snow sensitive to small amounts of absorbing impurities and in the near-infrared wavelengths, ice is more absorptive making albedo dependant primarily on grain size (Warren, 1982). Spectral variation in the reflectances of snow and cloud is the absorption coefficient that varies tremendously by the order of seven magnitudes in the wavelengths from 0.4 to 2.5 μm (Dozier, 1989).

Properties of snow are used as a basis for an automatic snow mapping procedure (Dozier, 1989). The Moderate Resolution Imaging Spectroradiometer (MODIS) on NASA Earth Observing System (EOS) platform, is ideal for monitoring snow cover extent due to its high spatial resolution (500 m), high spectral resolution (ranging from 0.4 to 2.5 μm wavelength), and frequent global coverage.

1.3 Binary and Fractional Snow Cover Mapping Approaches

Two approaches designed for MODIS have been widely used for mapping snow covered area (SCA) from satellites: (i) binary snow mapping algorithm that maps a pixel (an individual element of a picture) as either 0% or 100% snow-covered and (ii) fractional snow mapping algorithm that computes the fraction of a pixel that is covered by snow, with discrete values ranging from 0-100%.

Furthermore, other variations and improvements in snow mapping have been undertaken, and despite the efforts there are still limitations to the global mapping of snow cover in situations where mixed pixels occur. For example, mapping snow cover in forested regions is complicated due to the obscuring of snow cover by forest canopies, which results in the underestimation of the snow cover (Klein et al., 1997); the snow covered forested landscape is never completely snow covered because usually the top of tree canopy is partially or completely snow free. Furthermore, determining SCA in rugged terrain and high relief areas is more difficult than in areas with smoother topography, as the snow line is not well defined because of scattered snow patches (Seidel and

Martinec, 2004). In order to tackle these problems, advancements in snow mapping techniques are necessary and must be validated for future use.

The goal of this study is to compare a binary and a fractional method to determine snow percentage within a pixel. For this comparison, the MODIS binary snow mapping algorithm (Hall et al., 1995, Klein et al., 1997), and an enhanced fractional snow cover mapping algorithm that also uses MODIS data (Painter et al., 2003), are used. The MODIS binary snow mapping algorithm uses at-satellite reflectances in MODIS bands 4 (0.545–0.565 μm) and 6 (1.628–1.652 μm) to calculate the normalized difference snow index (NDSI):

$$NDSI = \frac{\rho_4 - \rho_6}{\rho_4 + \rho_6} \qquad (1)$$

The high reflectance of snow in the visible compared to the mid-IR wavelengths yields high NDSI values for snow compared to other surface materials. Hence, the NDSI is the basis for snow detection in the binary algorithm. A pixel is mapped as snow if the NDSI $\geq$ 0.4 and MODIS band 2 (0.841–0.876 μm) is > 11 %. Threshold value of 0.4 is effective in discriminating snow from non-snow and clouds (Dozier, 1989). MODIS Band 2 is used to prevent pixels containing liquid water that may have high NDSI values from being mapped as snow (Hall et al., 1995). As a result pixels will not be mapped as snow if the MODIS band 4 reflectance is <10%, even when other criteria are met (Hall et al., 2002). In order to decrease the probability of missing the SCA under densely covered forests, a vegetation correction is included by incorporating normalized difference vegetation index (NDVI) (Hall et al., 2002). The NDVI is an index of vegetation greenness derived from satellite images and can be used as an indicator of relative biomass and greenness (Tucker et al., 1985):

$$NDVI = \frac{\rho_{NIR} - \rho_{red}}{\rho_{NIR} + \rho_{red}} \qquad (2)$$

NDVI ranges from -1.0 to 1.0, with higher index values associated with greater vegetation cover. Snow and clouds will decrease NDVI values in some cases resulting in negative NDVI values. In dense forests, if NDVI $\simeq$ 0.1, the pixel may be mapped as snow covered even if the NDSI is < 0.4 (Hall et al., 2002).

The main limitation of the MODIS conventional snow-mapping algorithm is that it is a binary algorithm that maps a pixel as either snow or no snow. In many regions, snow abundance is effected by rock and vegetation cover. In cases where the snow is patchy within a pixel, this model either over or underestimates snow cover (Hall, 2002).

In the attempt to account for patchiness within a pixel, or mixed pixels, subpixel mapping of snow cover has been developed using spectral mixture analysis that allows the estimation of subpixel constituent areal fractions (Adams et al., 1986). The reflectance of an image pixel holds information about the number of constituents or end-members in a pixel, their spectral signatures, and their relative abundances. An endmember is a pure representation of a surface cover type with a distinctive spectral signature, such as snow, rock, or vegetation. A linear mixture model is based on the equation (Adam et al., 1986),

$$R_c = \sum_{i=1}^{N} F_i R_{i,c} + E_c \tag{3}$$

where, R_c is the apparent reflectance in sensor channel c; F_i is the fraction of end member i; $R_{i,c}$ is the reflectance of end-member i in channel c; N is the number of spectral end-members; and the fit of the linear mixture model to the spectral data in each pixel is measured by the error term E_c. The linear spectral mixture approach has been used in mapping SCA in alpine regions with multispectral instruments such as AVIRIS (Nolin et al., 1993) and Landsat Thematic Mapper (Rosenthal and Dozier, 1996). A single snow endmember, as used by these previous studies, may not be adequate since grain size gradients of snow can produce a range of spectral signatures (Painter el al., 1998).

With that in mind, a new enhanced model has been developed to map the snow cover at the fractional pixel level using Airborne Visible/Infrared Imaging Spectrometer (AVIRIS), and is called the Multiple Endmember Snow-Covered Area and Grain Size (MEMSCAG) (Painter et al., 2003). The algorithm uses multiple endmember spectral mixture analysis to simultaneously solve for subpixel snow cover and its grain size (Robert et al., 1998). Grain size is the snow parameter that determines its spectral albedo in the near-infrared wavelengths, while absorbing impurities. Model-derived grain-size estimates coupled with an estimate of impurity concentration can be used to estimate the albedo of the fractional snow cover (Warren, 1982). All previous grain size algorithms have the constraint that each pixel analyzed must have complete snow cover. Because the spectral reflectance of snow decreases with increasing grain size, multiple snow endmembers of different grain sizes are necessary to characterize the snow. Hence, in this model, the mixed-pixel problem is accommodated by determining the grain size of the fractional snow cover. Subscene spatial heterogeneity is addressed by allowing the number of endmembers and the endmembers themselves to vary pixel-by-pixel (Painter et al., 2003). A similar model that uses the same approach and is aimed at providing an accurate estimate of snow cover for regional studies in mountain areas has been developed for MODIS data. MODIS snow Covered Area and Grain Size/Albedo (MODSCAG) is used to obtain the fractional images from MODIS images (Painter et al., 2003).

In addition, several techniques for mapping fractional SCA that account for the effect of forest canopies overlying snow cover have been developed (e.g. Vikhamar and Solberg 2003, Metsamaki et al., 2005). Relatively, little is known about the effects of the forest canopy on mapping fractional snow covered area. Further comparison of the two approaches with quantitative assessment of effects of vegetation on measured SCA is needed.

1.4 Objectives/Hypotheses:

The main objectives of this study are to map snow cover extent accurately at a subpixel level, to examine the impact of vegetated and non-vegetated areas on SCA, and to test and validate new techniques that could be applied for future research work. Two hypotheses are proposed:

(1) Fractional snow cover mapping provides a more accurate estimate of snow covered area, as it maps SCA at subpixel resolution.

(2) Vegetation density affects snow cover mapping and will influence the results of the two methods to different degrees.

2 RESEARCH METHODS

2.1 Study Area

Two study regions were chosen: Sagarmatha National Park (also known as Everest National Park) and Annapurna Conservation region, both situated in Nepal (Figure 1). A regional scale of 1000 km^2 is used instead of the local watershed scale of 100 km^2 in order to better understand the spatial variability of snow cover. The Everest study region covers an area of 7200 km^2, with elevations ranging from 2000 m to 8840 m (at the summit of Mount Everest). The Annapurna study region covers an area of 7500 km^2, with elevation ranging from 1000 m to 8091 m (at the top of Annapurna Mountain). Both of these areas can be divided roughly into three elevation zones: vegetated lower zone, middle zone of alpine scrub and an upper alpine zone with permanent snowline (Jefferies, 1986).

The lower elevations of the Himalayan range have been denuded, which has greatly impacted the hydrology of that environment. A study done by Byers (2005) showed that the Mt. Everest region suffers from over harvesting of fragile alpine shrubs and plants for expedition and tourists lodge fuel, overgrazing, accelerated erosion, and uncontrolled lodge building (Byers, 2005). Land cover in Everest region consists of shrubby vegetated land to barren land at lower elevations and patchy snow covered area to deep snow cover at high elevation. Although deforestation is also apparent in the Annapurna study region, an innovative plan called the Annapurna Conservation Area Project has been set up to try to control the problem and to provide an alternative to continued deforestation. This project has been expected to serve as a globally relevant model of ecological sustainability and environmental protection (Stott, 1989). Hence, in Annapurna region, the land cover ranges from relatively more heavily vegetated lands at low elevations to deep snow cover at the high elevations.

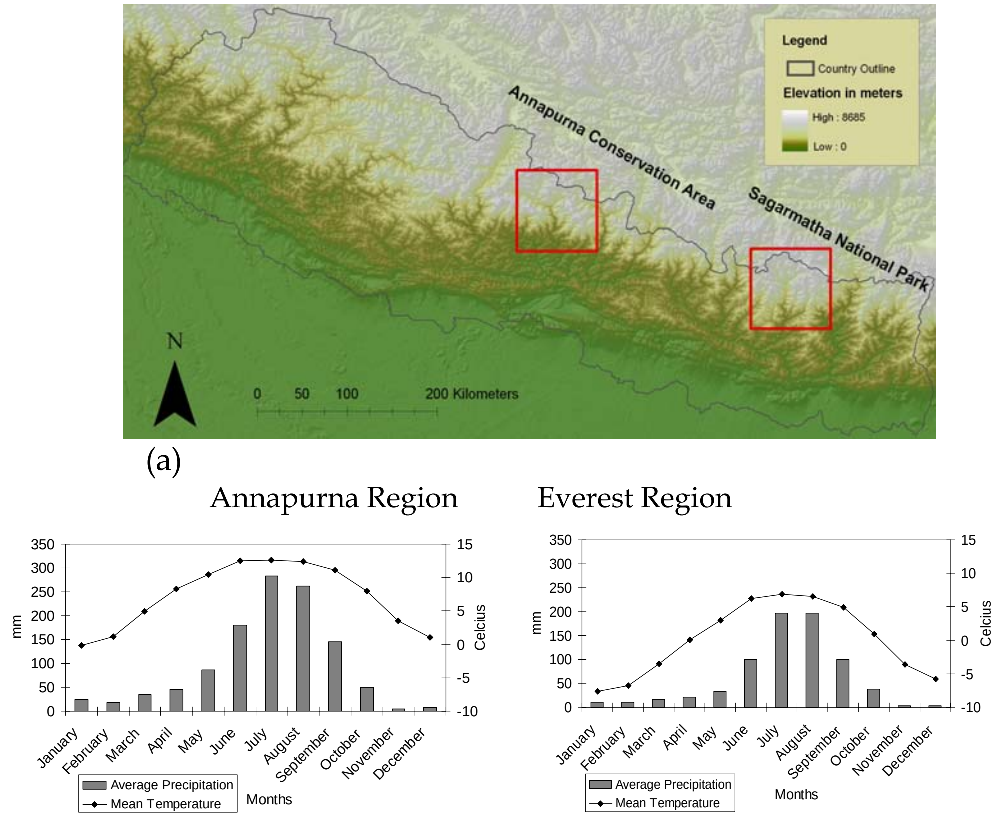

(b) (c)

Figure 1 (a) Study regions, Annapurna Conservation Area and Sagarmatha National Park (Everest National Park), (b) Climographs of Annapurna Conservation Area and (c) Climographs of Everest National Park (Source: generated using climate grids obtained from http://worldclim.org).

The climate of the study regions is dominated by the monsoon climate system with wet summers and cold, dry winters (Figure 1). Winter months extend from October to February when temperatures drop steadily from ~ -4° C to ~ -2° C. January until late March is usually one of long clear periods, temperature begin to increase during late March to April and May is often quite hot and brings an increase of pre-monsoon cloud cover with a few rain showers. The high peaks receive most of their snow during the monsoon season that extends from June and July and takes on a winter-like appearance with snow falling to about 5500 m (Jefferies, 1986). Therefore, snow accumulation generally occurs during the monsoon months extending through the winter months up until March, and snow ablation occurs during the months of April and May. Both study regions experience a similar climate pattern. In general, the Annapurna study region experiences warmer and wetter conditions than does the Everest study region (Figure 1).

2.2 Required MODIS Data

In 1999, NASA launched MODIS as part of the first EOS platform. Global maps of land surface properties, including snow cover, are created from MODIS images. Seasonal images for five years at 250 meters resolution of MODIS daily reflectance (MOD09) and MODIS binary images (MOD10A1) were collected based on criteria of cloud-free and nadir images. The MODIS reflectance images were used to generate the MODSCAG images with the help of the MODSCAG algorithm developed by Tom Painter et al., (2003). The months of March, April and May were critical in snow accumulation and ablation analyses, because the greatest change in accumulation and ablation of snow happens during these months due to high temperature gradient altering the snow phases (Barnett et al., 2005). Nadir images were used because less snow in forests will be imaged at off-nadir view angles and to minimize distortions in pixel geometry and anisotropic reflectance effects. Similarly, cloud-free images were preferred since the binary algorithm overestimates cloud cover and the MODSCAG algorithm does not have a built-in cloud mask.

A 90 m resolution Digital Elevation Model (DEM) was obtained from the Shuttle Radar Topography Mission (SRTM) dataset. The DEM was used in conjunction with the snow cover mapping technique to calculate the SCA along an elevation gradient that ranged from about 2500 m to about 7500 m, and at eight different aspects. Increments of 100 m in elevation and eight different aspects were aggregated to quantify the SCA obtained from the binary and the MODSCAG methods. MODIS 16 day NDVI (MOD 13 A1) images for May 2000, May 2001, May 2002, May 2003 and May 2004 were acquired to examine the vegetation effect on SCA. The month of May was chosen as a representative year for which to calculate NDVI values, since there was not much variation in NDVI values between the months in a year.

2.3 Data Processing

All images were subset to the required extent and georeferenced using the MRT (MODIS Reprojection Tool, Land Processes DAAC USGS Center for Earth Resource Observation and Science). Binary, MODSCAG, NDVI and SRTM images for all of the corresponding years were stacked as four individual layers and rescaled to 90 m using the ENVI 4.0 (The Environment for Visualizing

Images, Research Systems Inc. 2003) software. The unfinished SRTM data have significant data gaps, especially at higher elevations caused by radar shadowing in steep terrain. Therefore, these data gaps were masked in all other images during processing. In the various scenes of both the study regions, cloud covered areas are visible especially at lower elevations. Attaining completely cloud-free images during March – May was a challenge and cloud contamination in some of the images was unavoidable. Therefore, pixels that were mapped as cloud in the MODIS binary snow images were also mapped as cloud in the corresponding MODSCAG images in order to exclude them from the image analysis and reduce the errors that may be associated with their presence.

The two snow cover techniques were compared in elevation intervals of 100 m increments and for eight different aspects. Statistical analyses were performed to test for significant differences between the SCA produced by the binary and the MODSCAG techniques. Since these samples came from the same original images, the Student's Paired t-test with two samples was used to determine if the means of SCA were equal for both the techniques. To compare these two methods and to determine whether the variabilities for both methods were the same, the F-test was performed for the Everest as well as the Annapurna region. These comparisons are discussed in detail in the results section.

2.4 Validation of the MODSCAG Algorithm Using Landsat ETM+

Snow covered area and vegetation effects were validated using cloud-free Landsat Enhanced Thematic Mapper (ETM+) images. The higher spatial resolution of the Landsat sensor (30m) compared to MODIS (500m) makes it possible to distinguish snow from features and to determine their respective area in each elevation zone (Dozier, 1989). The absence of field data against which to compare binary SCA and MODSCAG SCA necessitated reliance upon images derived from Landsat ETM+, in lieu of direct observations. Two Landsat ETM+ images of the Everest study region for the dates March 10, 2002 and May 13, 2002, and one of the Annapurna study region for April 03, 2000 were used for the analysis. The paucity of these data is due to availability of cloud-free images, dates of the Landsat images that correspond closely to the dates of the MODIS images, and to some extent the cost associated in obtaining these data. Preprocessing of the Landsat ETM+ images included converting from top of atmosphere radiance to at-sensor reflectance (Chander and Markham, 2003). Landsat images were then atmospherically corrected using the dark pixel subtraction method (Chavez, 1998).

Validation using the Landsat ETM+ data was performed in two ways. First, the NDSI was calculated using Landsat ETM+ reflectance band 2 (0.52-0.60 µm, green) and Landsat ETM+ band 5 (1.55-1.75 µm, mid-infrared). The Landsat image was processed using the same criteria used in the MODIS binary snow classification, where a pixel was mapped as snow if the NDSI $\geq$ 0.4 and MODIS band 2 (0.841–0.876 μm) > 11 %. The resulting SCA maps generated from Landsat ETM+ were compared with binary SCA and MODSCAG SCA of the same date. The second validation approach used multiple bands of Landsat ETM+ and was classified using the Iterative Self-Organizing Data Analysis Technique (ISODATA). ISODATA is a widely used unsupervised classification and uses iterative algorithms by clustering algorithm which makes a large number of passes through the remote sensing dataset (Jensen, 1996). A gray scale image of binary and MODSCAG scenes, and a four band (red, green, blue and NIR) of Landsat ETM+ were used for the classification. Seven classes were generated, which were simplified into two classes that were identified as a snow and a snow-free class by visual inspection. The classified Landsat images were compared with the corresponding binary and MODSCAG images.

3 RESULTS AND DISCUSSIONS

3.1 Comparison of Binary and MODSCAG SCA Based on Elevation

SCA computed from the MODIS binary snow technique and the MODSCAG technique were compared against each elevation range. The SCA generated from both these techniques were normalized by the total area within each elevation increment and converted to percent SCA. The year 2000 for both the Everest study region and the Annapurna study region was used as a representative year for discussion since the other four years exhibited similar general pattern of SCA at different elevation zones and at different aspects. Figures 2 and 3 show percent SCA derived from binary and MODSCAG methods along with mean NDVI plotted as a function of elevation for the year 2000. Mean NDVI was calculated as an average NDVI over each 100 m interval. Mean SCA was calculated using the average SCA of all the seasons for both the techniques. Figures 4 and 5 show the difference plot of binary and MODSCAG SCA. Tables 1 and 2 show the areal extent of snow cover computed by each method for the four elevations zones of the Everest study region and Annapurna study region respectively; the statistically different means are shown in bold.

The results of the SCA (based on elevation) for both regions show that percent SCA from the binary algorithm and from the MODSCAG algorithm increased with increase in elevation. NDVI, on the other hand, decreased with increase in elevation for the study regions. Both study regions show similar trends, with increasing percent snow cover varying directly with increase in elevation. The following subsections detail the mapping results for each elevation increment.

3.1.1 Lower < 4000 m

At elevations below 4000 m, the Everest region shows no significant difference between binary SCA and MODSCAG SCA, although, in general, the binary algorithm mapped slightly less land as snow cover with mean SCA of 42 km^2 than did the MODSCAG method with mean SCA of 51 km^2 (Table 1). Likewise, in the Annapurna region, the binary method mapped slightly less snow cover, with mean SCA of 130 km^2, than did the MODSCAG technique with mean SCA of 147 km^2 (Table 2). The statistical analyses show that there is no significant difference in variance and no significant difference in the means of SCA produced from the binary and the MODSCAG algorithms at this elevation range.

Interestingly, in some of the images, the binary technique mapped more SCA at the lower elevation than did the MODSCAG. This is evident at the Annapurna region for the month of March in all years (Figures 3 and 5). This phenomenon is observed only at this lower elevation range where NDVI values are high. One possible explanation of such pattern is due to the incorporation of NDVI in the binary algorithm, which mapped higher snow cover during the accumulation period in March. With NDVI values of approximately 0.4, the Annapurna study region represented more vegetation than did the Everest study region, with NDVI values of approximately 0.2. In the subsequent months of April and May, melting of snow later in the month may have resulted in more patchy snow cover beneath the forested canopy and may have produced lower binary SCA and more MODSCAG SCA at this lower elevation zone. If such is the case, then the binary technique appears to characterize the vegetated landscape better, since snow is likely to be present beneath the vegetation during the accumulation phase.

3.1.2 Middle 4000 m to 5000 m

At middle elevations between 4000 m – 5000 m, at both regions, MODSCAG mapped more land as snow cover than did the binary method. For the Everest region, mean SCA produced by binary was 445 km^2, versus the MODSCAG SCA of 487 km^2 (Table 1). For the Annapurna region, mean SCA produced by the binary algorithm was 723 km^2 , versus 769 km^2 of SCA produced from the MODSCAG algorithm (Table 2). The test of equal variance between two methods at this elevation range resulted in no significant difference, however the test of equal means resulted in a significant difference in the means of SCA.

Compared to the lower elevation range results, the NDVI values for the Everest study region remained at about 0.2 while NDVI values for the Annapurna region decreased from 0.4 to about 0.2, which could represent a similar land cover type of scrubby vegetation and patchy snow cover common to both. Higher percent SCA produced by the MODSCAG algorithm and lower percent SCA obtained from the binary algorithm also suggests the inhomogeneity of the land cover within each pixel (Figures 2 and 3). For these heterogeneous areas of incomplete and patchy snow covered area, MODSCAG may very well have provided better results than the MODIS binary snow cover technique because the latter assumes 100% snow cover for pixels with 50% or more snow cover.

3.1.3 Middle-to-higher 5000 m - 6000 m

At middle-to-higher elevations of about 5000 m – 6000 m, SCA from both techniques mapped similar proportions of land as snow, with a mean binary SCA value of 1319 km^2 and a mean MODSCAG SCA value of 1318 km^2 for the Everest region (Table 1), and a mean binary SCA value of 950 km^2 and a mean MODSCAG SCA value of 923 km^2 for the Annapurna region (Table 2). The shift in trend in the percent SCA from binary and MODSCAG algorithms is evident at this elevation range; above this range, binary SCA started to map more snow, and MODSCAG, less snow cover (Figures 2 and 3). There is no significant difference in the variances of the two methods and in the difference in the means of SCA produced from both the techniques.

At this elevation range, the NDVI dropped below zero in all cases representing permanent snow cover with no vegetation cover. Hence, at this elevation range between 5000 m – 6000 m, the homogeneity of the snow-covered land area is well represented. The similarity in the SCA mapped by both the binary and the MODSCAG technique is because of absence of mixed pixels. Most of the pixels in this range did not have varied land cover features present within each pixel, but rather snow occupied most of the landscape representing continuous snow cover within each pixel.

3.1.4 Upper > 6000 m

Above 6000 m altitude, where high peaks and permanent snow cover prevail at both study regions and for all seasons, the binary product consistently mapped a higher percentage of the study area as snow covered than did the MODSCAG product (Figure 4 and 5), with mean binary SCA of 455 km^2 versus mean MODSCAG SCA of 394 km^2 (Table 1) for Everest, and mean binary SCA of 230 km^2 versus mean MODSCAG SCA of 212 km^2 for Annapurna (Table 2). At these higher elevation ranges, the variances between the two methods is still not significant, however, the means of SCA from both the products is significantly different.

Overall, both the techniques mapped a higher percentage of snow cover above 6000 m than at lower elevations, and less than zero NDVI, indicating permanent snow cover (Figures 2 and 3). However, the lower percentage of SCA mapped by MODSCAG may have represented the landscape more accurately. Snow frequently slides off the steep slopes by avalanches or is blown off the ridges resulting in snow-free patches exposing bare rocks. The MODSCAG fractional SCA mapping appears to capture this heterogeneity, providing more accurate snow cover mapping in such cases.

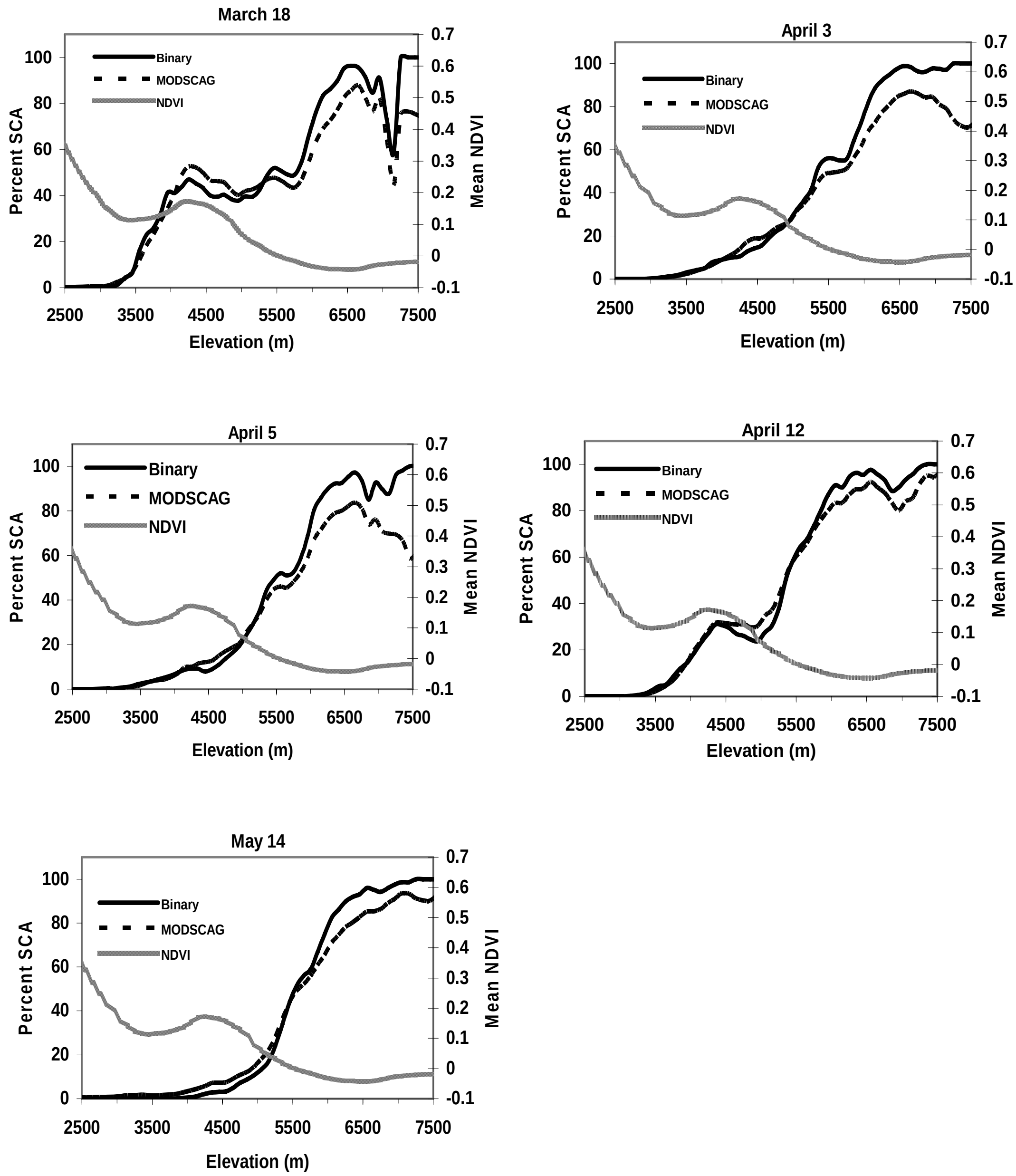

Figure 2 Percent SCA of the Everest region derived from the binary and the MODSCAG methods along with the mean NDVI plotted as a function of elevation for the year 2000.

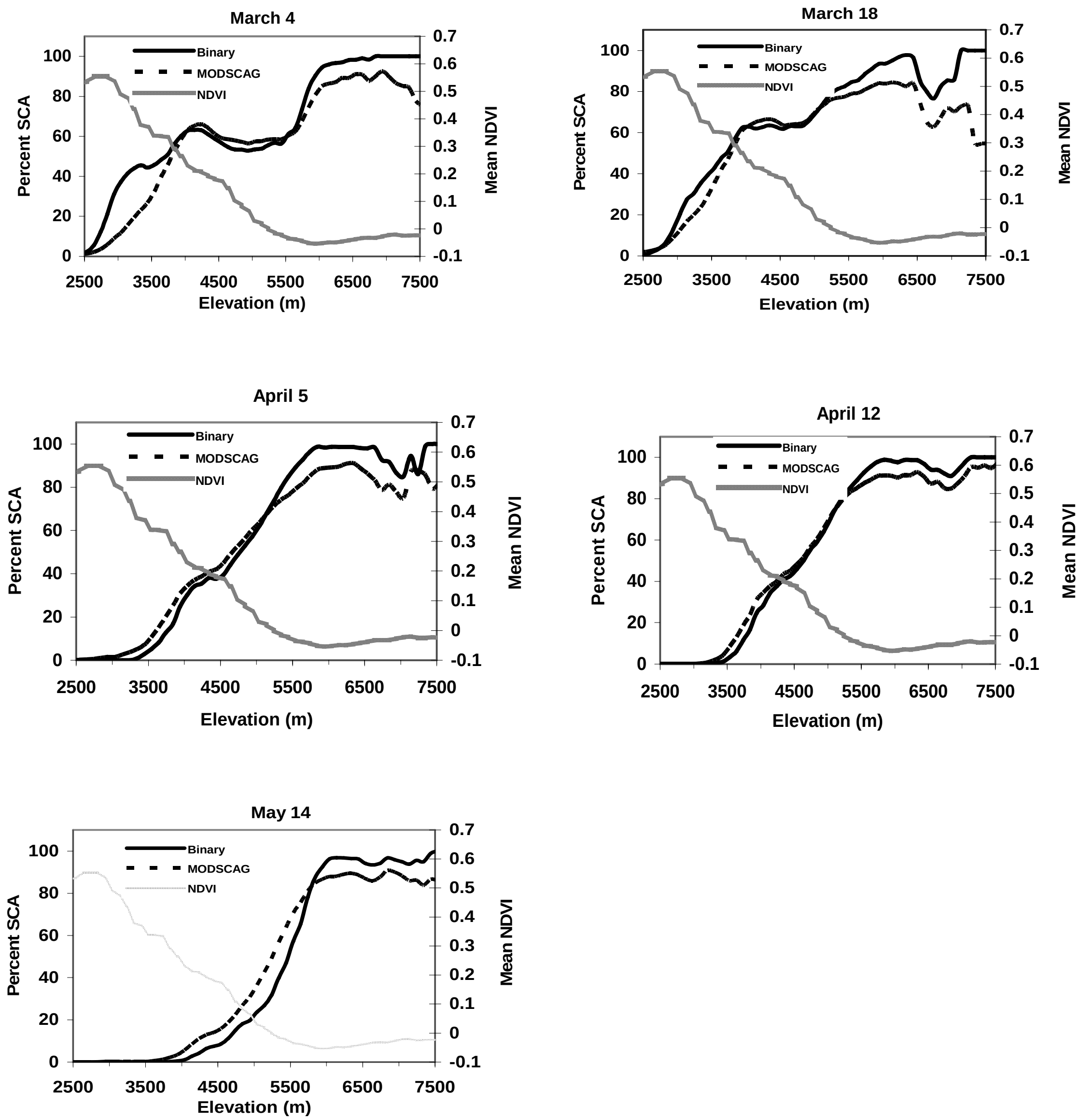

Figure 3 Percent SCA of the Annapurna region derived from the binary and the MODSCAG methods along with the mean NDVI plotted as a function of elevation for the year 2000.

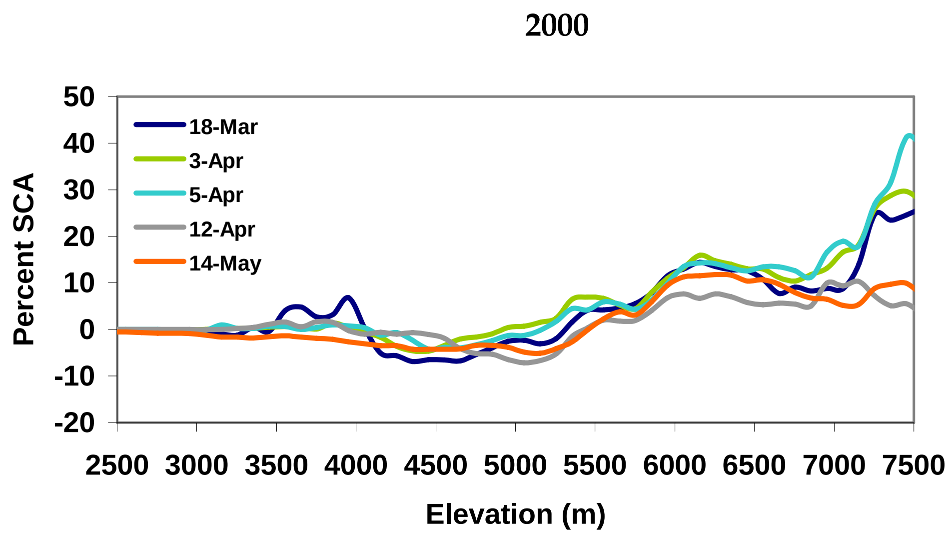

Figure 4 Difference plots of percent binary SCA and percent MODSCAG SCA for the year 2000 at the Everest region.

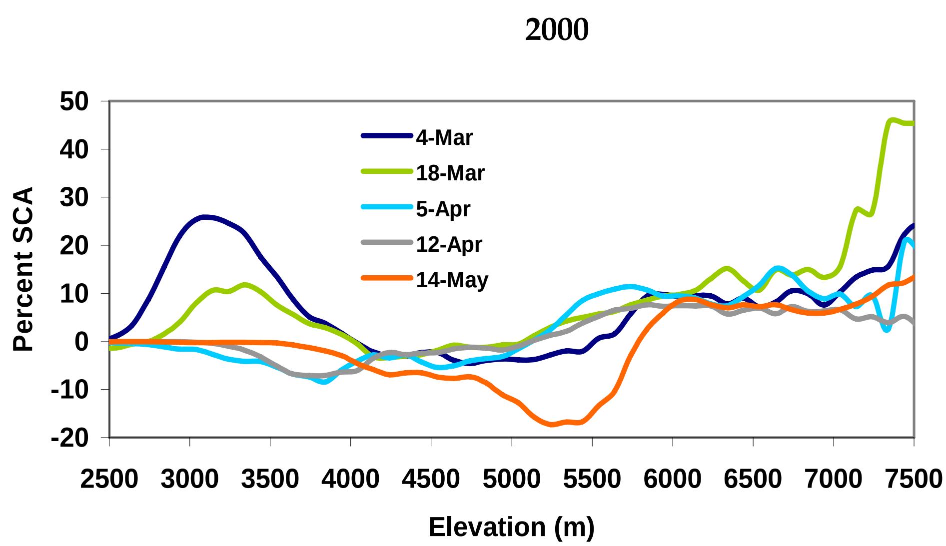

Figure 5 Difference plots of percent binary SCA and MODSCAG SCA for the year 2000 at the Annapurna region.

Table 1 Area of snow cover computed by each method for the four elevation zones of the Everest study region. Sample populations with statistically different means are shown in bold.

Date	SCA (km^2)								Cloud in the image (%)
	Lower zone (4000 m)		Middle zone (4000 - 5000 m)		Middle-to-upper zone (5000 - 6000 m)		Upper zone (6000 m)		
	Binary	MODSCAG	Binary	MODSCAG	Binary	MODSCAG	Binary	MODSCAG	
2000									
4-Mar	78	68	344	452	1118	1072	448	386	24
18-Mar	125	103	638	714	1211	1216	442	374	17
3-Apr	28	25	298	355	1163	1168	469	395	7
5-Apr	21	17	200	238	1051	1056	456	383	10
12-Apr	38	32	410	466	1381	1386	484	447	8
21-Apr	14	20	134	206	918	999	396	355	21
14-May	2	18	93	152	1004	1009	461	403	14
2001									
12-Mar	36	53	225	313	1156	1161	442	370	27
16-Mar	98	84	567	593	1204	1209	333	275	12
1-Apr	41	54	714	780	1595	1600	463	387	18
8-Apr	1	9	184	246	1068	1073	440	367	20
22-Apr	1	72	350	420	1584	1465	488	425	23
24-Apr	31	45	442	475	1320	1325	467	409	7
2002									
10-Mar	82	73	865	829	1509	1514	463	391	9
19-Mar	40	52	558	613	1507	1512	464	394	12
2-Apr	57	45	453	600	1635	1583	464	406	29
18-Apr	6	27	266	346	1212	1217	458	396	7
2-May	1	34	443	519	1620	1625	483	424	14
4-May	23	55	492	519	1502	1507	469	422	10
2003									
4-Mar	142	106	995	881	1557	1562	468	408	10
11-Mar	85	90	1002	988	1582	1587	408	335	19
20-Mar	212	178	1191	1118	2062	1974	495	448	23
12-Apr	25	45	340	432	1478	1389	462	399	23
14-Apr	12	35	542	606	1702	1707	502	470	13
5-May	8	24	381	405	1303	1308	467	394	11
7-May	6	10	282	307	1150	1155	459	390	9
16-Mar	16	47	151	197	990	972	435	378	21
2004									
9-Apr	12	20	93	131	608	732	438	379	33
16-Apr	0	8	114	152	830	835	433	372	7
3-May	61	102	490	534	1359	1364	495	416	6
Mean of all dates	42	51	**445**	**487**	1319	1318	**455**	**394**	

Table 2 Area of snow cover computed by each method for the four elevation zones of the Annapurna study region. Sample populations with statistically different means are shown in bold.

Date	SCA (km^2)								Cloud in the image (%)
	Lower zone (4000 m)		Middle zone (4000 - 5000 m)		Middle-to-upper zone (5000 - 6000 m)		Upper zone (6000 m)		
	Binary	MODSCAG	Binary	MODSCAG	Binary	MODSCAG	Binary	MODSCAG	
2000									
4-Mar	523	343	819	861	608	611	169	143	8
18-Mar	334	284	927	953	942	896	125	105	16
3-Apr	105	155	671	672	802	715	148	134	20
5-Apr	70	119	643	702	972	905	205	185	12
12-Apr	88	139	834	878	1130	1090	266	247	1
21-Apr	12	33	289	372	612	586	192	145	29
14-May	1	12	166	289	658	818	284	260	5
2001									
12-Mar	94	114	765	853	1233	1216	276	261	20
16-Mar	477	411	1340	1408	1265	1247	282	264	3
1-Apr	20	50	413	409	654	618	58	75	32
8-Apr	49	97	746	834	1169	1123	285	268	6
24-Apr	23	69	702	830	1109	1156	316	269	7
2002									
10-Mar	406	396	1520	1472	1429	1277	303	276	2
19-Mar	177	240	1185	1244	1368	1225	312	279	3
2-Apr	186	235	1395	1323	1374	1315	263	228	14
18-Apr	17	82	460	561	683	670	165	139	13
2-May	18	94	548	599	867	794	168	142	12
4-May	14	64	592	764	1107	1138	310	268	21
2003									
4-Mar	287	276	1064	1044	1096	983	188	390	22
11-Mar	230	161	561	572	606	567	125	102	25
20-Mar	295	276	1275	1304	1311	1248	261	234	6
5-Apr	104	127	880	832	1056	987	219	168	20
12-Apr	49	102	759	802	1222	1177	312	298	8
14-Apr	5	50	280	363	597	613	202	189	18
5-May	115	139	954	902	1096	1007	214	199	14
7-May	11	38	226	287	316	289	69	59	24
16-May	1	23	285	384	850	944	302	277	23
2004									
9-Apr	2	15	214	291	607	689	252	215	21
16-Apr	1	19	225	287	573	636	291	257	3
3-May	178	244	966	969	1175	1147	327	295	5
Mean of all dates	130	147	**723**	**769**	950	923	**230**	**212**	

3.2 Comparison of SCA based on Aspect

Results from the comparison of SCA computed from the MODIS binary snow product and the MODSCAG product by aspects are illustrated in Figures 6 and 7. For both regions SCA produced from the binary and the MODSCAG products behaved similarly when analyzed using eight aspects (north, northeast, east, southeast, south, southwest, west, and northwest). Overall, the binary product mapped more snow cover than the MODSCAG product.

From Figures 6 and 7 suggest that the southwest and west facing slopes exhibit the fastest depletion in the SCA compared to the northeast and east facing slopes. Snow is affected mostly by solar radiation and high solar intensity, and consequently produces more melt later in the day. Hence, depletion of snow cover occurred faster on southwest and west facing slopes than on northeast and east facing slopes. Both the binary and the MODSCAG SCA techniques are able to show this phenomenon. This examination of SCA demonstrates that the binary SCA and MODSCAG SCA are good ways to derive and to quantify the snow cover from satellite images.

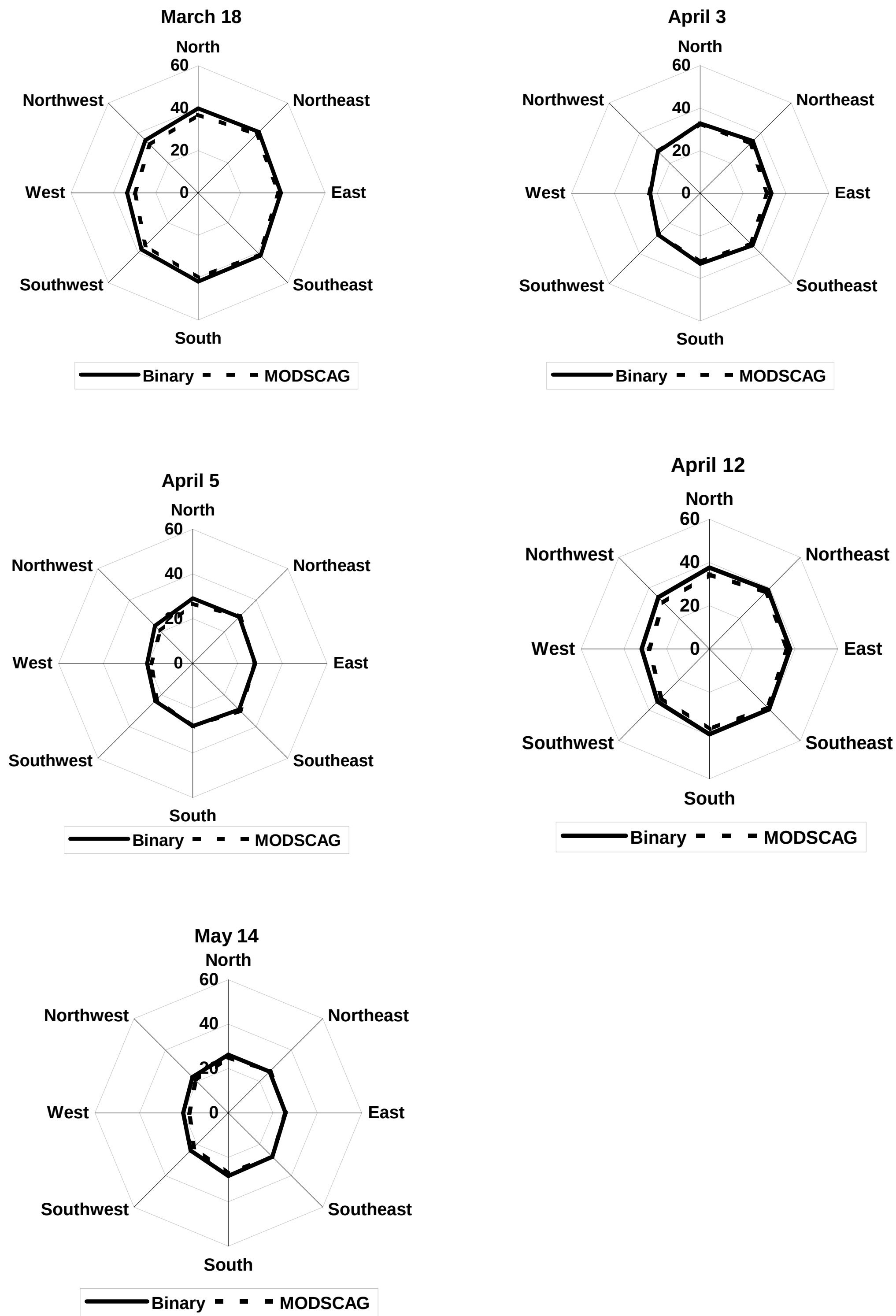

Figure 6 Binary and MODSCAG SCA of the Everest region computed at eight different aspects for the year 2000.

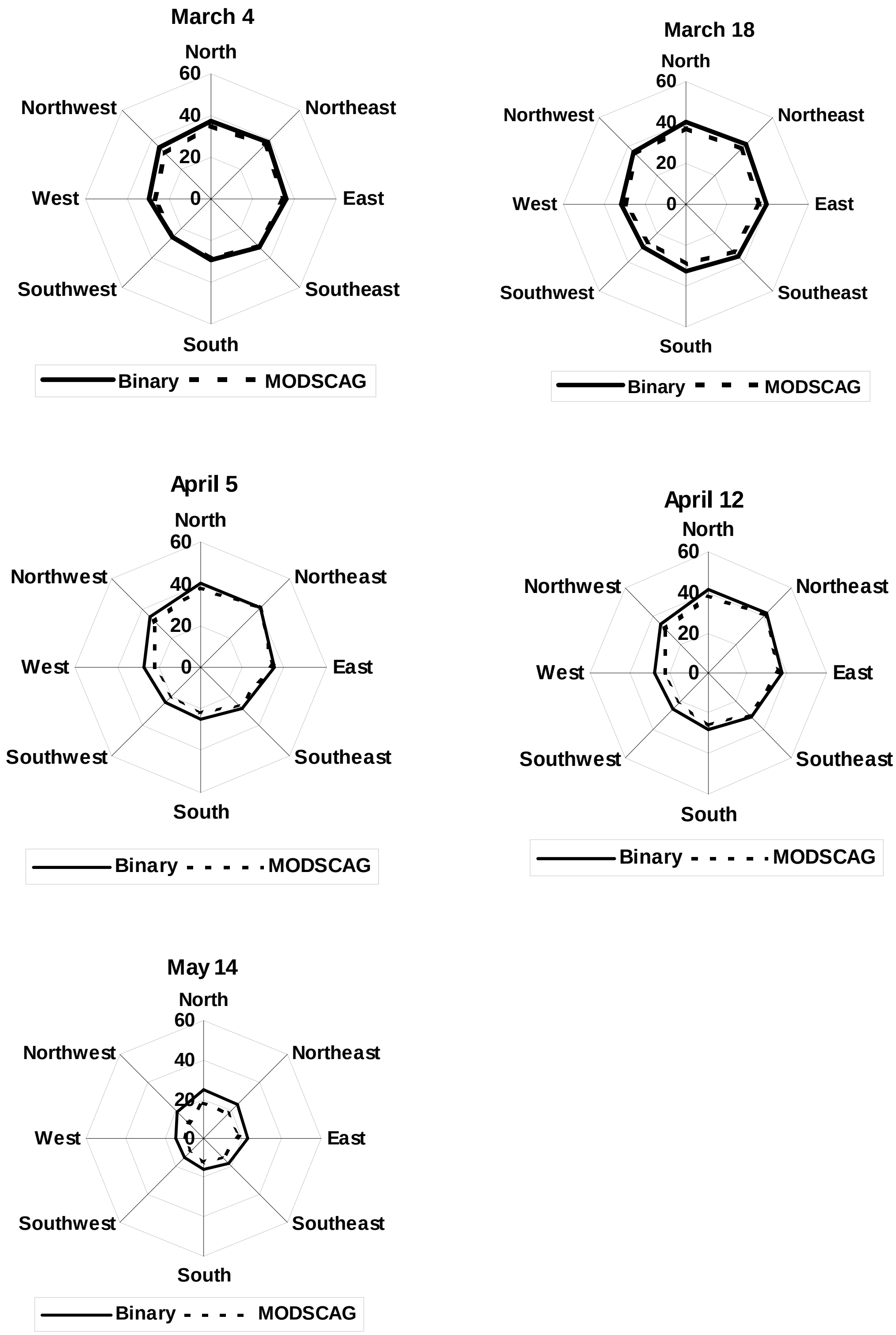

Figure 7 Binary and MODSCAG SCA of the Annapurna region computed at eight different aspects for the year 2000.

3.3 Time Sequence of Snow Cover Maps

A gradual decrease of the snow covered area is a typical feature of the snow cover at elevation where seasonal snow cover occurs. Sequence of snow cover maps, represents a quantitative measure in time and space of the dynamically changing snow cover during the melting season. This is a valuable source of information as they serve as a quantitative measure of the snowmelt recession behavior. The time sequence maps are helpful in showing the general trend in the snow processes during the peak accumulation and ablation process. These maps provided further analysis of change in SCA between the binary and the MODSCAG product as seasons progressed.

The time sequence maps for the Everest study region and the Annapurna region for the year 2000 is chosen as a representative year (Figures 8 and 9). The year of 2004 showed slight variations compared to the other years due to the incorrect processing of MODIS reflectance image for May 3 2004, hence will be disregarded. Images that had the least cloud contamination (less than 20 %) were visually inspected to understand the spatial pattern of snow covered area and predict the depletion time of snow covered area. The onset of snow melt can be observed in the month of April with peak melt later in the month and in the month of May. This analysis shows that the binary and the MODSCAG products are quite effective in displaying the dynamic spatial distribution of the snow covered area.

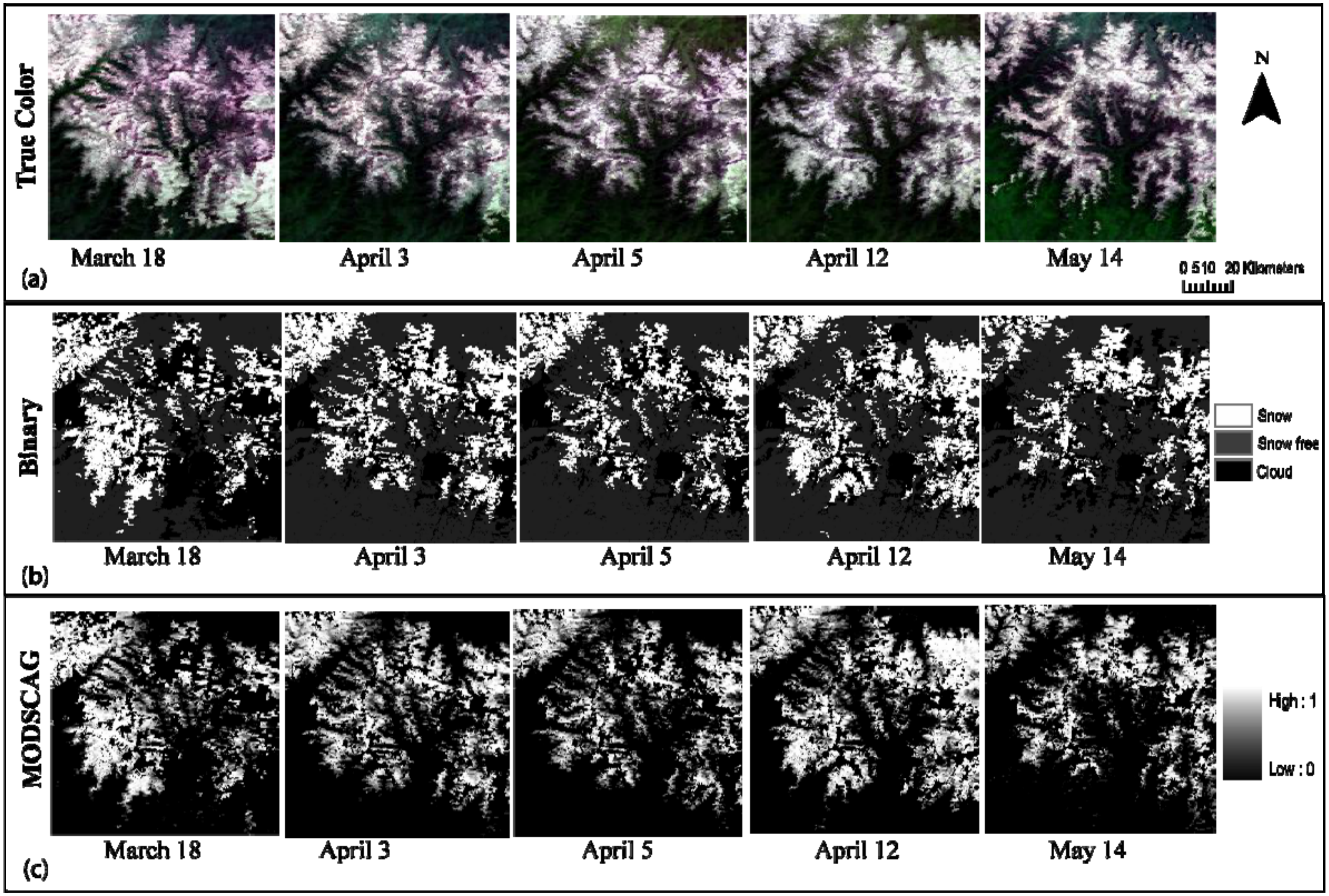

Figure 8 Time sequence maps of the Everest region shown in the MODIS true color, the binary SCA and the MODSCAG SCA images of the year 2000.

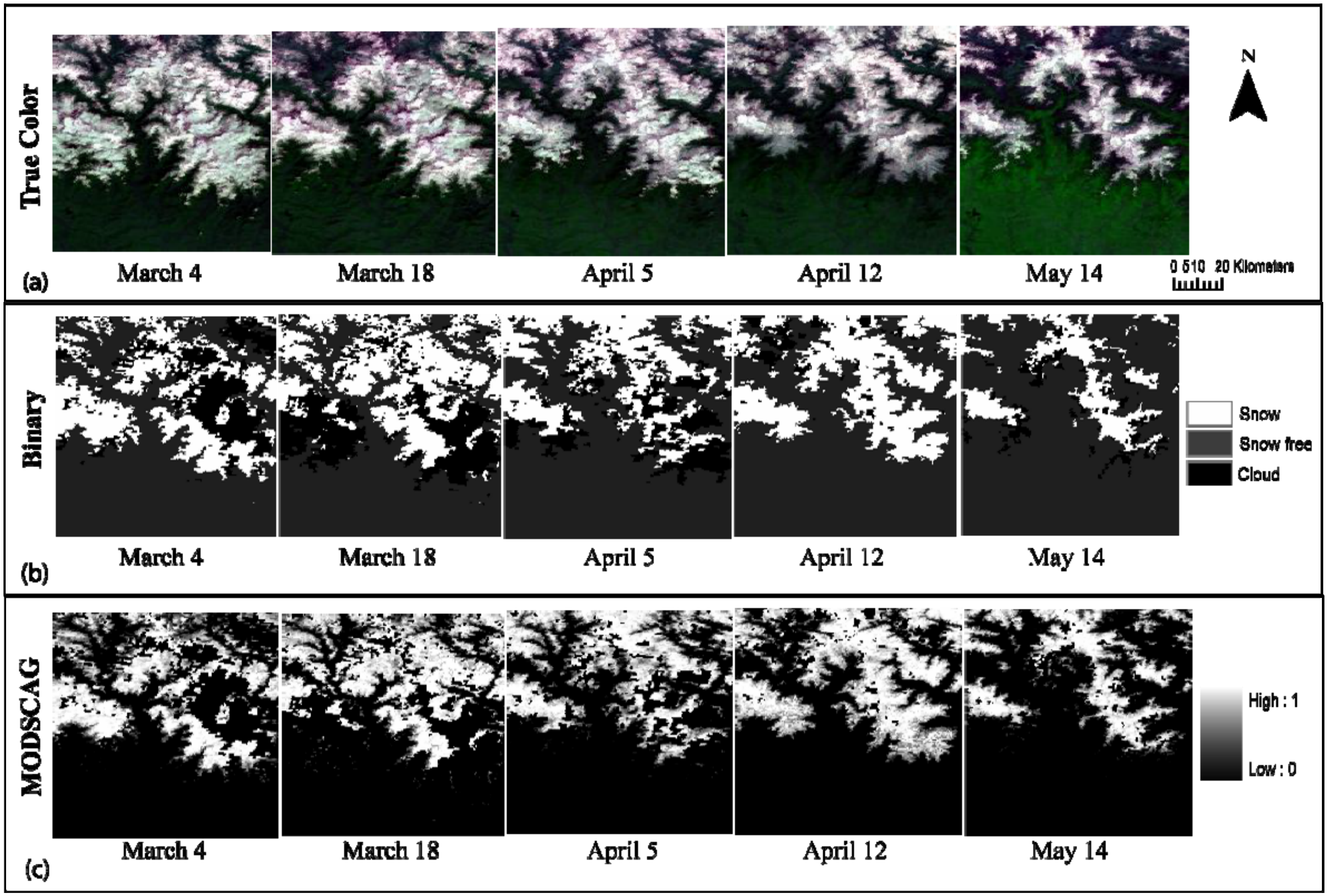

Figure 9 Time sequence maps of the Annapurna region shown in the MODIS true color, the binary SCA and the MODSCAG SCA images of the year 2000.

3.4 Validation Using Landsat ETM+

The results from the comparison of Landsat ETM+ SCA with the MODIS binary and the MODSCAG images of the same dates show that the MODSCAG technique is more effective at estimating snow cover at higher elevations. SCA generated using the Landsat ETM+ imagery and both binary and MODSCAG SCA followed a similar trend (Figures 10-12). For the Everest study region, on March 10, 2002, the Landsat ETM+ NDSI values closely matched the MODSCAG SCA. For May 13, 2002, NDSI calculated from Landsat ETM+ was less than the other two techniques throughout the elevation range from 2500 m to 7500 m. However, it was closer to the MODSCAG SCA, especially at the higher elevation range. A closer look reveals that at elevations where snow cover is patchy, MODSCAG characterized the landscape better than did binary (Figure 13). Also at high elevation where bare rocks are exposed due to high wind and steep terrain, MODSCAG effectively characterized the heterogeneous land cover.

Unsupervised classification reveals that the MODSCAG snow classification compared well with the Landsat ETM+ snow classification (Figure 14). Change detection statistics conducted on classified images for the Everest study region reveal that for March 10, 2002, 82% of SCA obtained from binary classification is correctly classified as snow versus 88% of SCA obtained from MODSCAG, when both classified images are compared to the Landsat ETM+ classification. For May 13, 2002 of the Everest region, a classified image of binary snow compared with a classified image of Landsat ETM+ show weaker results, with 70% correctly classified as SCA. A more encouraging result is obtained when a classified image of MODSCAG snow cover was compared with a Landsat ETM+ classified image; 80% SCA is correctly classified. Likewise, when Landsat ETM+ classified image of April 3, 2000 of the Annapurna study region was compared with the binary classified image and the MODSCAG classified image of the corresponding date, the MODSCAG SCA was mapped closer to Landsat ETM+ classified image with 87% than the binary classified image with 86%. For all of three cases, the MODSCAG classified images compared better to the Landsat ETM+ classified images than did the binary classified images.

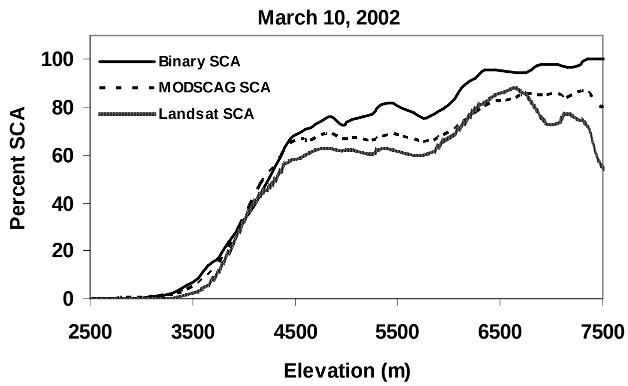

Figure 10 Percent SCA of the Everest region of Landsat ETM+ (dervied using the binary algorithm), binary SCA and MODSCAG SCA for March, 10, 2002.

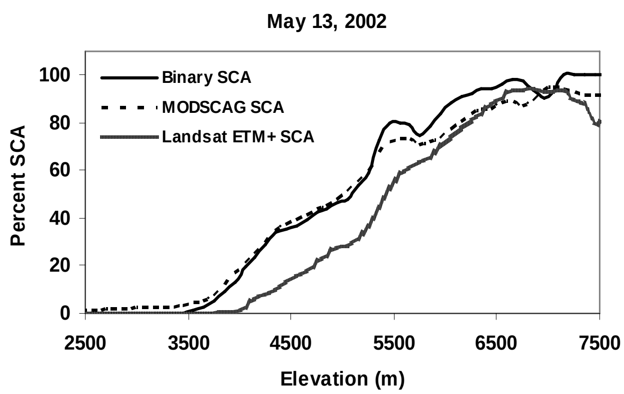

Figure 11 Percent SCA of the Everest region of Landsat ETM+ (dervied using the binary algorithm), binary SCA and MODSCAG SCA for May, 13, 2002.

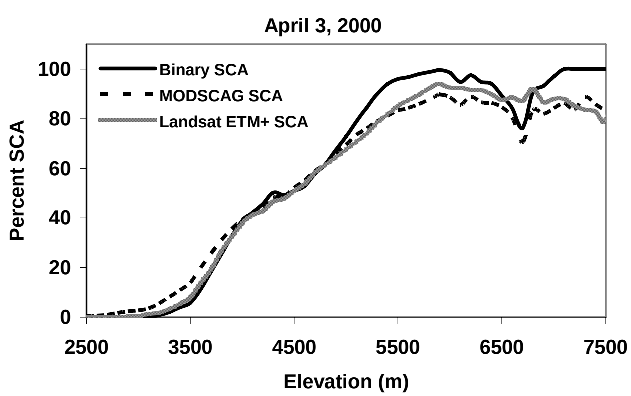

Figure 12 Percent SCA of the Annapurna region of Landsat ETM+ (dervied using the binary algorithm), binary SCA and MODSCAG SCA for April 3, 2002.

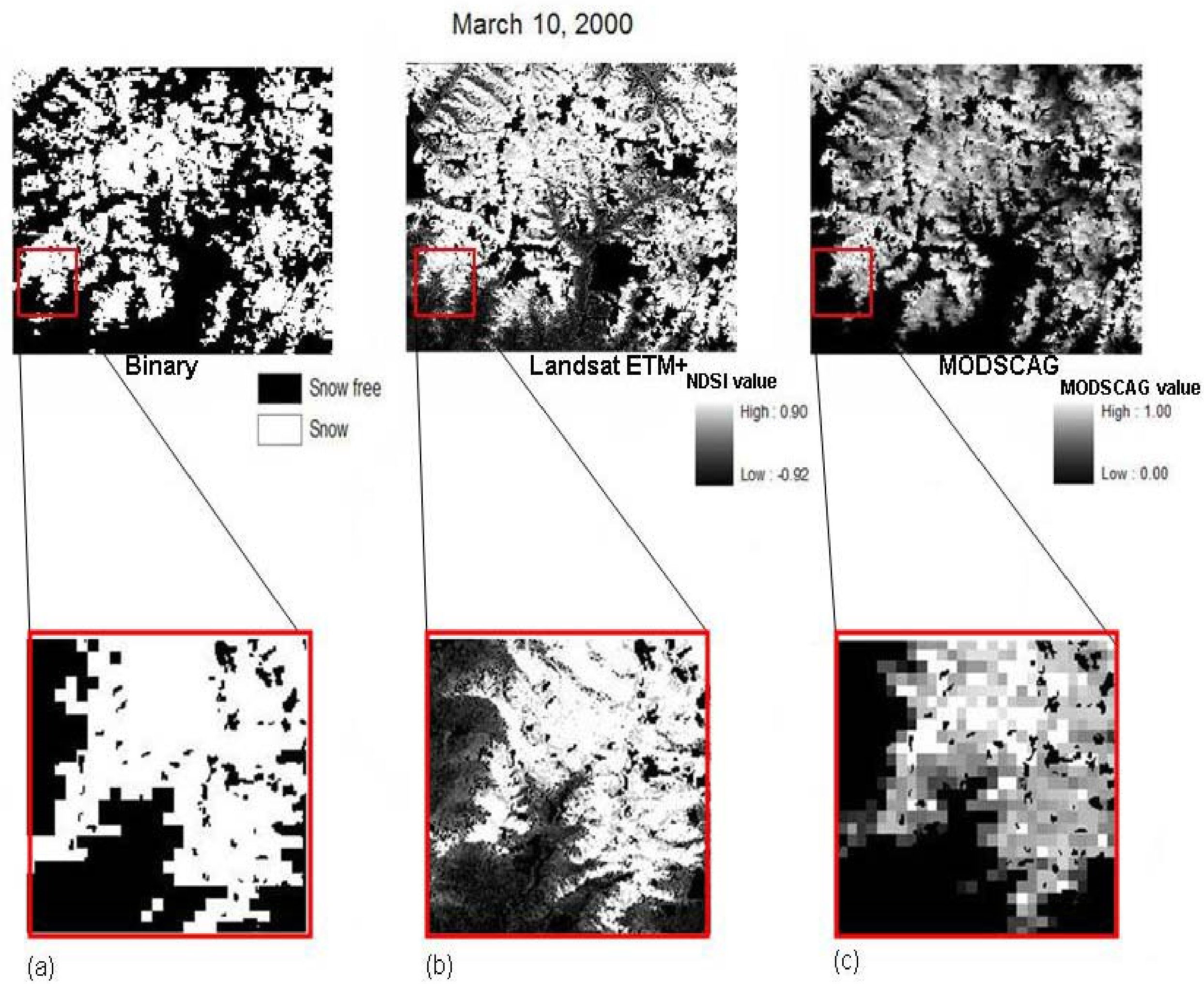

Figure 13 SCA maps of binary, Landsat ETM+ and MODSCAG images for March 10, 2000. A closer look at (a) Binary SCA (b) Landsat ETM+ SCA (c) MODSCAG SCA images. MODSCAG SCA closely matches with the Landsat ETM+ SCA.

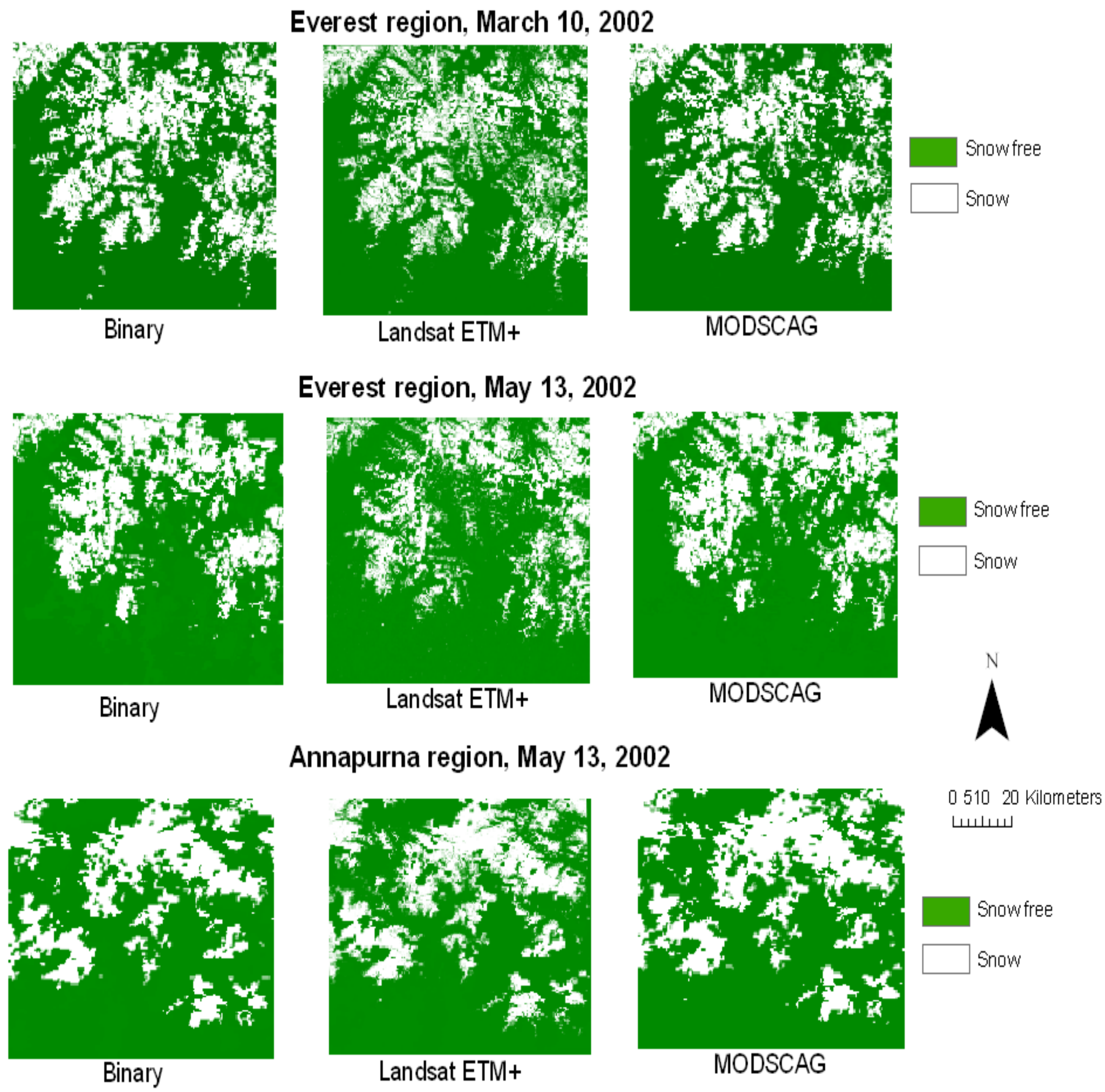

Figure 14 Classified images created using unsupervised ISODATA classification method on binary, Landsat ETM+ and MODSCAG images of the Everest study region and the Annapurna study region.

3.5 Error Analysis

Cloud cover in the study area prevented the correct estimation of SCA, since overestimation of clouds by the binary algorithm was a large source of error. Confusion in the identification of cloud over snow was experienced when modeling SCA in high elevation regions by the MODIS binary product (Hall et al., 2000). Cloud-contaminated pixels also prevented MODSCAG from accurately mapping the SCA. Additionally, unfinished SRTM data prevented an exact representation of SCA at higher elevations, since the gaps were present mainly at higher elevations. Moreover, errors associated with scaling were introduced with the scaling of 250 m resolution MODIS images to match the resolution of 90 m SRTM data for ease of analysis.

Absence of ground truth information data reduces the ability to draw quantitative conclusions regarding classification errors. There have been many recent studies evaluating snow-cover mapping techniques using satellite-derived data and all of these studies demonstrate difficulties in evaluating satellite-derived snow cover (Hall et al., 2000). Although, Landsat ETM+ was used to evaluate and validate the snow cover mapping techniques, it could have produced uncertainty in the validation results. Differences in spectral bandwidth of green and SWIR bands between Landsat ETM+ (0.525-0.605 μm and 1.55-1.75 μm) and MODIS (0.545-0.565 μm and 1.628-1.652 mm) when computing NDSI could have produced different results in different satellite images adding to the uncertainty of the validation results.

4 CONCLUSIONS

This paper compared two MODIS snow cover mapping techniques: (1) binary, and (2) fractional (MODSCAG). Differences in SCA between these two products was quantified and validated with Landsat ETM+. The binary snow cover mapping technique and MODSCAG mapping technique are both sufficient to produce an accurate snow cover map where there is a presence of homogeneous snow cover. However, snow cover at middle (4000 m – 5000 m) elevations and upper (> 6000 m) elevations was mapped differently depending on the technique used. The binary classification underestimated the low-elevation snow and overestimated the high-elevation snow. The MODSCAG product did a better job of estimating SCA at higher elevations (> 6000 m) and also in areas of heterogeneous land cover with fractional snow cover (4000-5000 m) due to the presence of other land features occurring within each pixel. While the binary product mapped nearly 100% of land at the elevation range of > 6000 m as snow, MODSCAG produced less snow cover at this elevation range. On the other hand, the binary technique may have been better at lower elevations during the accumulation season, due to the vegetation correction that MODSCAG did not have. For intermediate elevations (5000 m -

6000 m), both binary and MODSCAG performed similarly and produced an adequate result. Thus, the MODSCAG algorithm was comparatively better for mapping SCA at all elevation ranges except where an abundance of snow cover might be present underneath a dense forest canopy (usually towards lower end of the elevation range).

Using Landsat ETM+ images was an effective way of assessing the accuracy of the two techniques. It is important to be able to map the extent of snow cover as accurately as possible, especially in regions that depend on snow melt for water resources. Varied topography and complex land cover further complicate snow cover mapping. The results show that MODSCAG will increase the accuracy of mapping snow-covered area, and consequently will make better estimates of snow melt. This improved accuracy has hydrological implications. Snow cover at relatively lower elevations with patchy snow cover will melt earlier than snow cover at high elevations. Incomplete snow cover in the four elevation zones investigated for this study needs to be accounted for in order to improve predictions of runoff. Underestimation of SCA by the binary algorithm at these elevation ranges will result in lower melt water volume and inaccurate snowmelt predictions. However, during the accumulation period (month of March) at lower elevations, the binary SCA method may be of better use since it incorporates vegetation effects.

From a time sequence figure of snow cover maps of March to May (Figures 8 and 9), it is possible to roughly estimate the onset of snow melt and the peak melting period. Melt water production is directly proportional to the changing spatial extent of the seasonal snow cover. It is therefore of advantageous to exploit satellite monitoring instead of modeling the snow coverage from precipitation and temperature data to monitor seasonal changes in snow cover as seasons progress.

There is still need for further work in this field in order to improve the accuracy of remotely-sensed SCA. This paper illustrates the influence of vegetation cover as a complex and complicated issue in snow cover mapping using satellite sensors. In order to accurately estimate fractional SCA in forested and partially forested regions, the MODSCAG algorithm requires information on the effects of a wide range of forest canopy densities on mapped fractional SCA (Painter et al., 2003). Hence, development and incorporation of an algorithm to include the cloud mask and type, structure, and density of the forest canopy in order to provide an accurate estimate of snow cover underneath the canopy cover will greatly improve the fractional snow mapping algorithm.

This research provided preliminary results of the accuracy of the fractional snow cover mapping technique, MODSCAG, on mountain environments, while highlighting its deficiencies. Remote sensing by satellites provides a tool for monitoring dynamically changing snow coverages, and advances the remote mapping of snow in heterogeneous landscapes. Ultimately, it is hoped that such remote sensing investigations will improve the hydrological predictions in remote areas.

REFERENCES

Adams, J.G., Smith, M.O., and P.E. Johnson (1986), Spectral mixture modeling: A new approach to analysis of rock and soil types at the Viking Lander 1 site, *Journal of Geophysical Research*, 91, 8098-8112.

Barnett, T. P., Adam J. C., and D. P. Lettenmaier (2005), Potential impacts of a warming climate on water availability in snow-dominated regions, *Nature*, 438 (17), 303-309.

Byers, A. (2005), Contemporary human impacts on alpine ecosystems in the Sagarmatha (Mt. Everest) National Park, Khumbu, Nepal, *Annals of the Association of American Geographers,* 95 (1), 112-140.

Chalise, S.R., Kansakar, S., Gwyn, R., Croker, K., and M. Zaidman (2003), Management of water resources and low flow estimation for the Himalayan basins of Nepal, *Journal of Hydrology*, 282, 25-31.

Chander, G. and B. Markham (2003), Revised Landsat-5 TM radiometric calibration procedures and postcalibration dynamic ranges, *IEEE Transactions on Geoscience and Remote Sensing*, 41 (11), 2674-2677.

Chavez, P.S. Jr. (1988), An improved dark-object subtraction technique for atmospheric scattering correction of multispectral data, *Remote Sensing of the Environment*, 24, 459-479.

Dozier, J. (1989), Spectral signature of alpine snow cover from the Landsat Thematic Mapper, *Remote Sensing of Environment*, 28, 9-22.

Golding, D.L. and R. H. Swanson (1986), Snow distribution patterns in clearings and adjacent forest, *Water Resources Research,* 22, 1931-1940.

Hall, D. K. and A. B. Tait (2000), Intercomparison of satellite-derived snow-cover maps, *Annals of Glaciology*, 31, 369-376.

Hall, D. K. and J. Martinec (1985), Remote Sensing of Ice and Snow, Chapman and Hall Ltd., New York.

Hall, D. K., Riggs, G. A., and V.V. Salomonson (1995), Development of methods for mapping global snow cover using moderate resolution imaging spectroradiometer data, *Remote Sensing of Environment*, 54, 127-140.

Hall, D. K., Riggs, A. G., Salomonson, V. V., DiGirolamo, N. E., and K. J. Bayr (2002), MODIS snow cover products, *Remote Sensing of Environment*, 83, 181-194.

Hardy, J.P., Davis, R. E., Jordan, R., Ni, W., and C.E. Woodcock (1998), Snow ablation modeling in a mature aspen stand of the boreal forest, *Hydrological Processes,* 12, 1763–1778.

Hedstrom, N.R. and J.W. Pomeroy (1998), Measurements and modeling of snow interception in the boreal forest, *Hydrological Processes*, 12, 1611-1625.

Ichii, K., Maruyama, M., and Y. Yamaguchi (2003), Multi-temporal analysis of deforestation in Rondônia state in Brazil using Landsat MSS, TM, ETM+ and NOAA AVHRR imagery and its relationship to changes in the local hydrological environment, *International Journal of Remote Sensing*, 24 (22), 4467-4479.

Jefferies, M. (1986), Mount Everest National Park – Sagarmatha, mother of the universe, *The Mountaineers*, David Bateman Ltd, New Zealand.

Jensen, J.R. (1996), Introductory digital image processing: A remote sensing perspective, Prentice Hall, Englewood Cliffs, New Jersey.

Jordon, G. (1994), Mountain environments and geographic information systems - GIS modeling and model variation of deforestation risks in Sagarmatha National Park, Nepal, Taylor and Francis Publishers, London.

Klein, A. G., Hall, D. K., and G. Riggs (1997), Improving the MODIS global snow-mapping algorithm, Proceedings of IGARSS '97 – *International Geoscience and Remote Sensing Seminar*, 619-621.

Metsamaki, S.J., Anttila, S.T., Markus, H.J., and J.M. Vepsalainen (2005), A feasible method for fractional snow cover mapping in boreal zone based on a reflectance model, *Remote Sensing of Environment*, 95, 77-95.

Murray, C. D., and J.M. Buttle (2003), Impacts of clearcut harvesting on snow accumulation and melt in a northern hardwood forest, *Journal of Hydrology*, 271, 197-212.

Nolin, A. W., Dozier, J., and L.A.K. Mertes (1993), Mapping alpine snow using a spectral mixture modeling technique, *Annals of Glaciology*, 17, 121-124.

Painter, T. H., Roberts, D.A., Green, R.O., and J. Dozier (1998), The effect of grain size on spectral mixture analysis of snow-covered area from AVIRIS data, *Remote Sensing of Environment*, 65, 320-332.

Painter, T. H., Dozier, J., Roberts, D. A., Davis, R. E., and R.O. Green (2003), Retrieval of subpixel snow-covered area and grain size from imaging spectrometer data, *Remote Sensing of Environment* , 85, 64-77.

Rango, A. and J. Martinec (1979), Application of a snowmelt-runoff model using Landsat data, *Nordic Hydrol*., 10, 225-238.

Roberts, D. A., Gardner, M., Church, R., Ustin, S., Scheer, G., and R. O. Green (1998), Mapping chaparral in the Santa Monica Mountains using multiple endmember spectral mixture models, *Remote Sensing of Environment,* 44, 255-269.

Rosenthal, W., and J. Dozier (1996), Automated mapping of montane snow cover at subpixel resolution from the Landsat Thematic Mapper, *Water Resources Res*., 32(1), 115-130.

Seidel, K. and J. Martinec (2004), Remote sensing in snow hydrology runoff modelling, effect of climate change, Springer, Berlin.

Stevens, S.F. (2003), Tourism and deforestation in the Mt. Everest region of Nepal, *The Geographical Journal,* 169 (3), 255-277.

Storck, P., Lettenmaier, D.P., and S.M. Bolton (2003), Measurement of snow interception and canopy effects on snow accumulation and melt in a mountainous maritime climate, Oregon, United Sates, *Water Resources Research*, 38 (11), 1223-1239.

Stott, T. (1989), Deforestation in Nepal, *Geography Review*, 3 (1), 32-35.

Tucker, C. J., Townshend, J. G., and T. E. Goff (1985), African land-cover classification using satellite data, *Science*, 227 (4685), 369-375.

Vikhamar, D. and R. Solberg (2003), Snow mapping in forests by constrained linear spectral unmixing of MODIS data, *Remote Sensing of Environment*, 88, 309-323.

Warren, S.G. (1982), Optical properties of snow, *Reviews of Geophysical and Space Physics*, 20 (1), 67-89.

APPENDIX A: Percent SCA plots derived from the binary and the MODSCAG methods along with the mean NDVI plotted as a function of elevation.

Everest Study Region (2001)

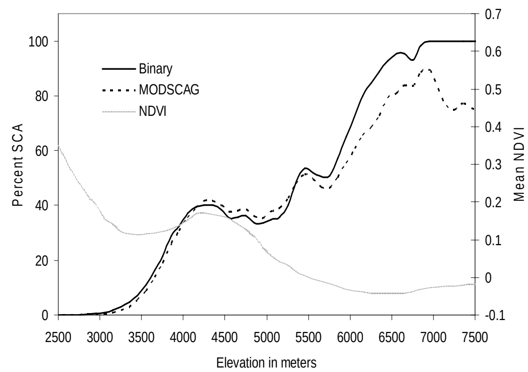

(a) March 16

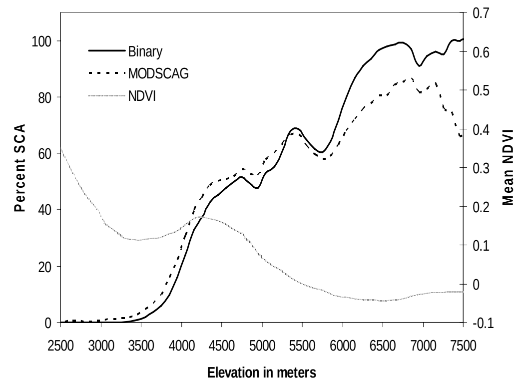

(b) April 1

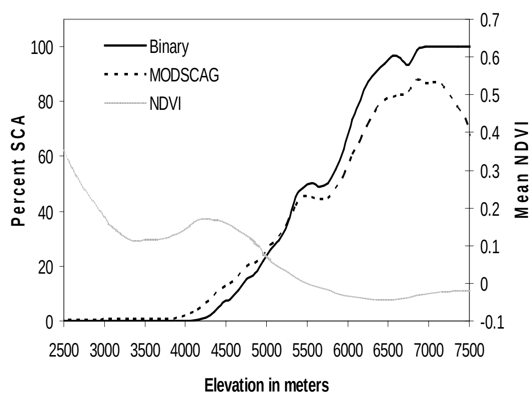

(c) April 8

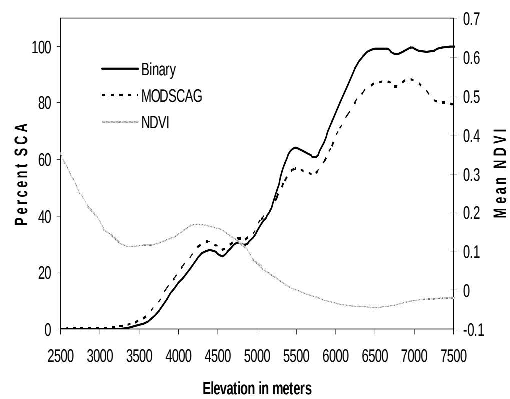

(d) April 24

Everest Study Region (2002)

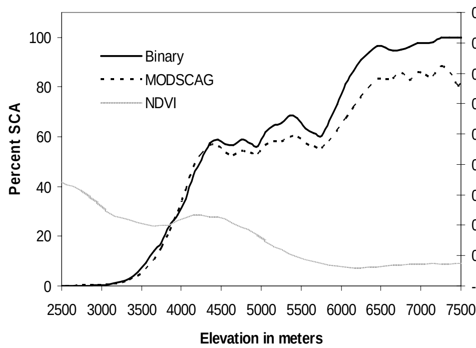

(a) March 10

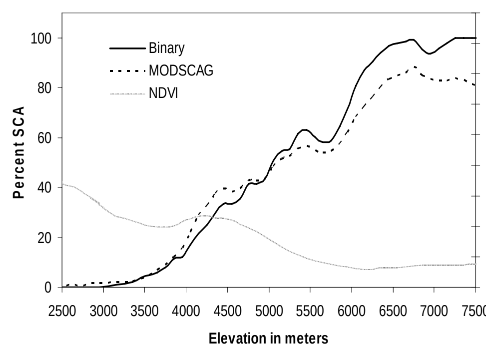

(b) March 19

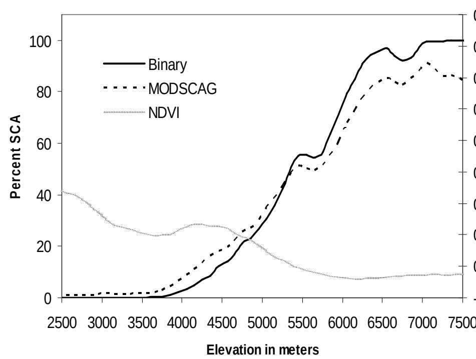

(c) April 18

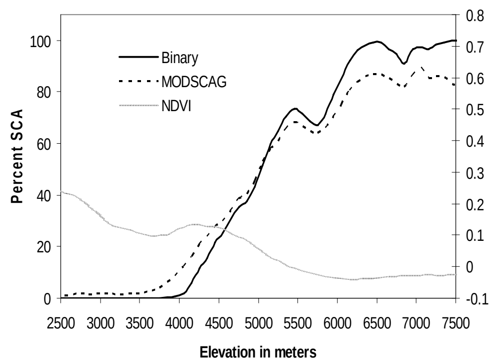

(d) May 02

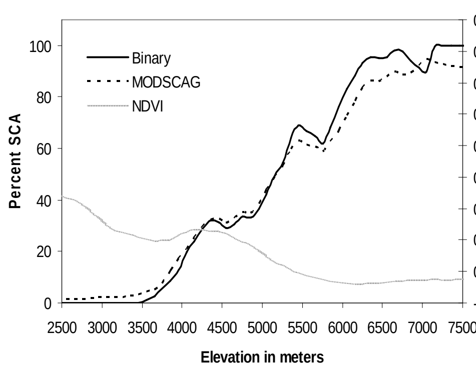

(e) May 04

Everest Study Region (2003)

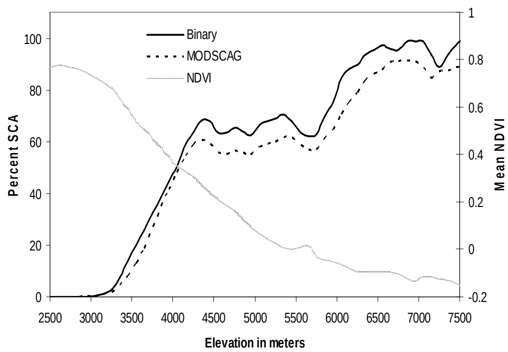

(a) March 4

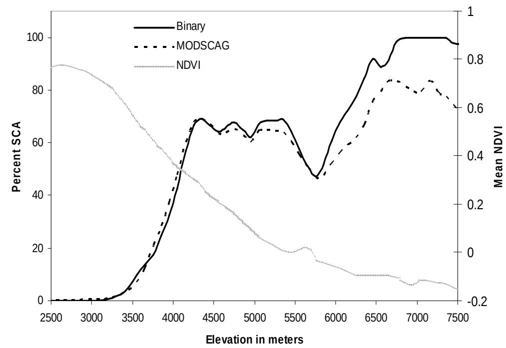

(b) March 11

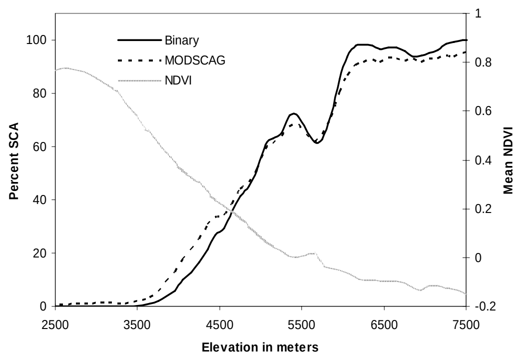

(c) April 14

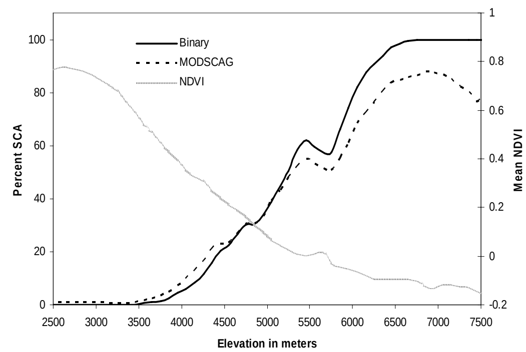

(d) May 5

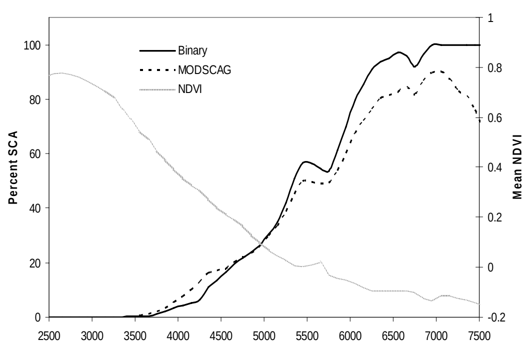

(e) May 7

Everest Study Region (2004)

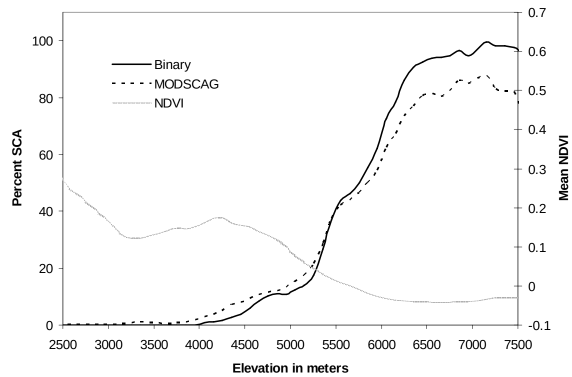

(a) April 16

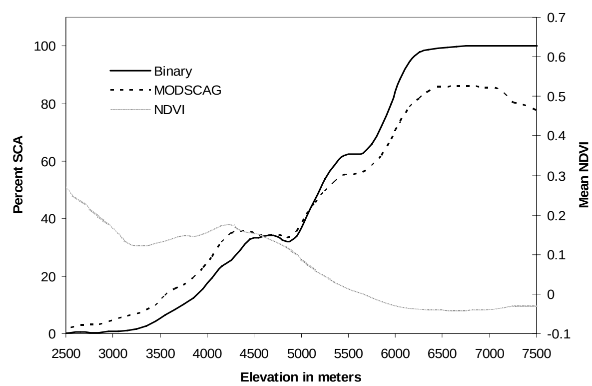

(b) May 3

Annapurna Study Region (2001)

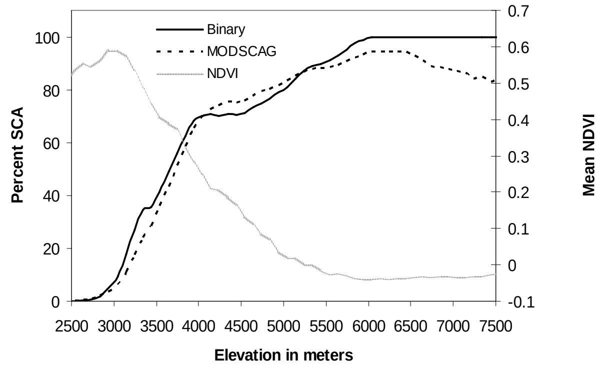

(a) March 16

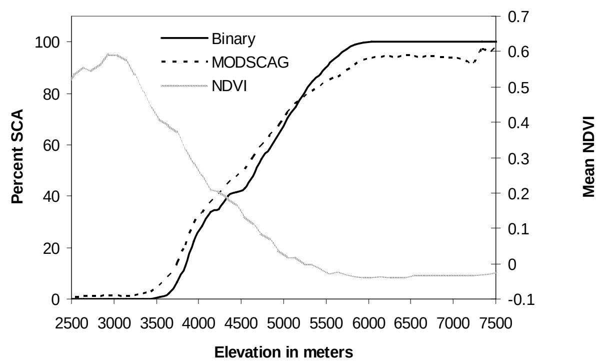

(b) April 8

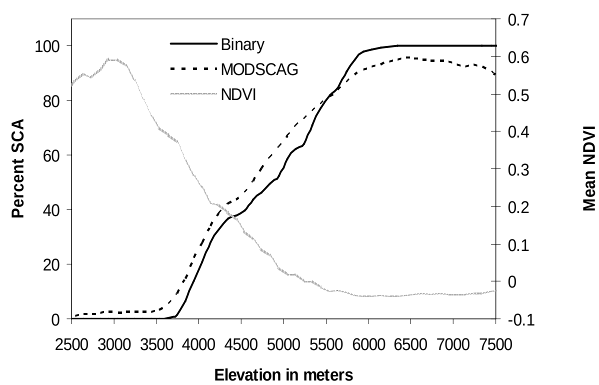

(c) April 24

Annapurna Study Region (2002)

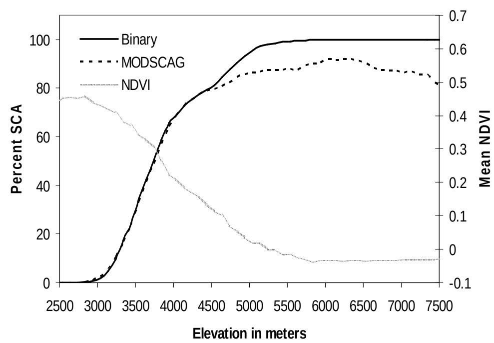

(a) March 10

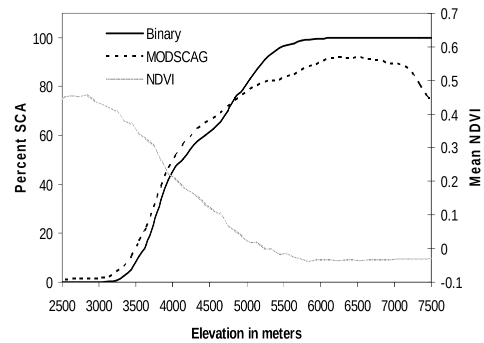

(b) March 19

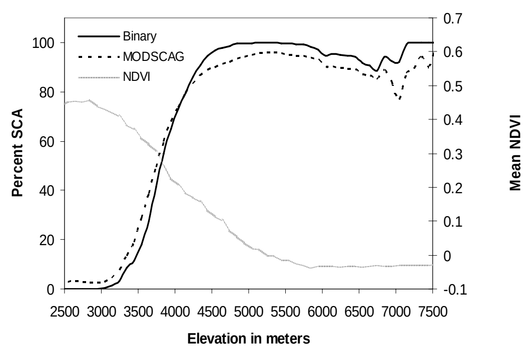

(c) April 2

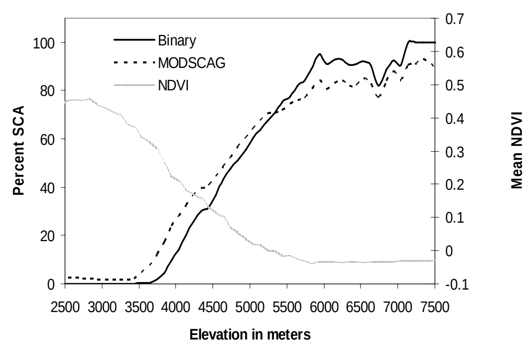

(d) April 18

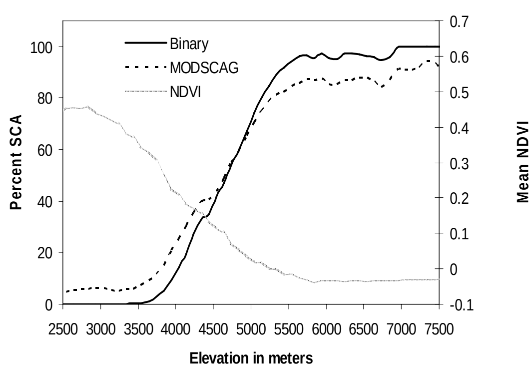

(e) May 2

Annapurna Study Region (2003)

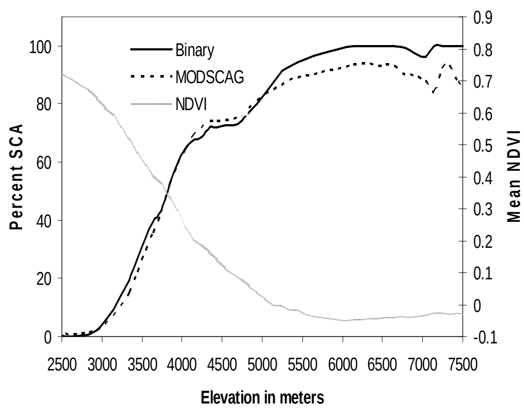

(a) March 20

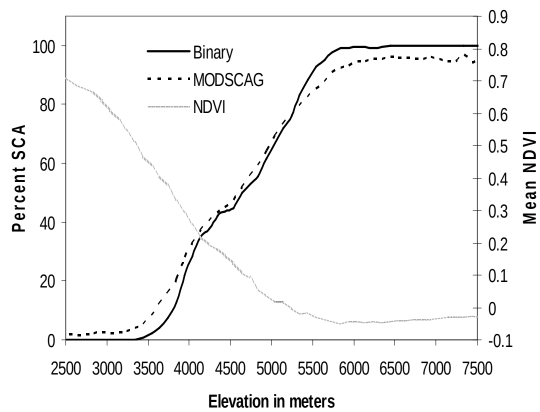

(b) April 12

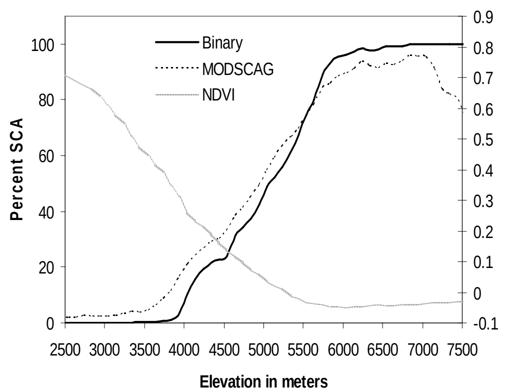

(c) April 14

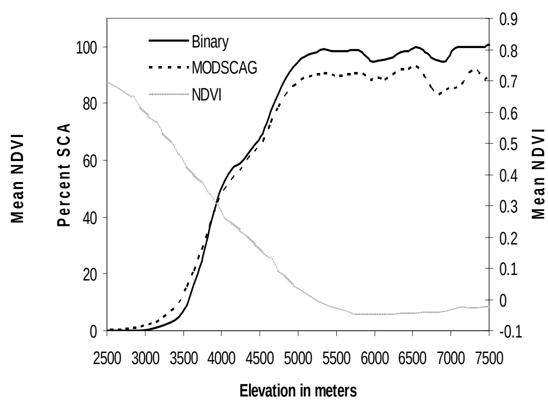

(d) May 05

Annapurna Study Region (2004)

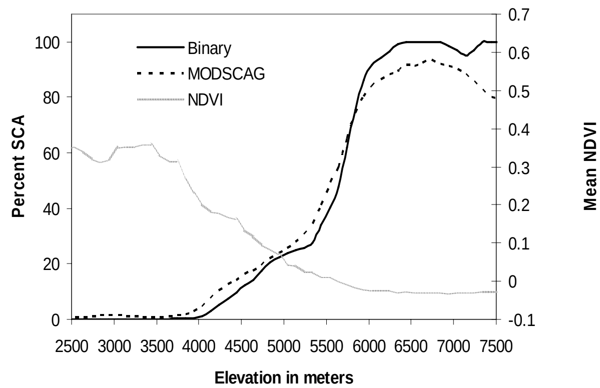

(a) April 16

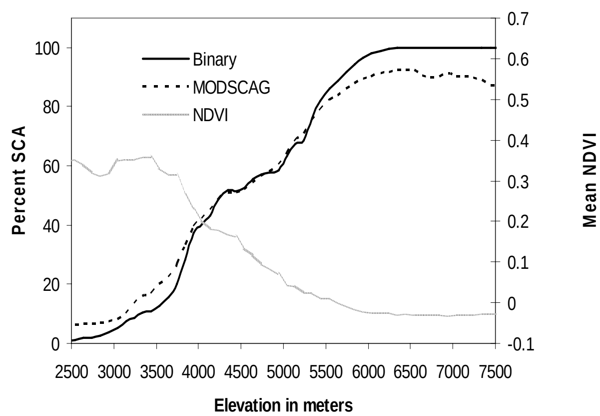

(b) May 3

APPENDIX B: Difference plots for the Year 2001, 2002, 2003 and 2004 of the Everest study region and the Annapurna study region.

Everest study region

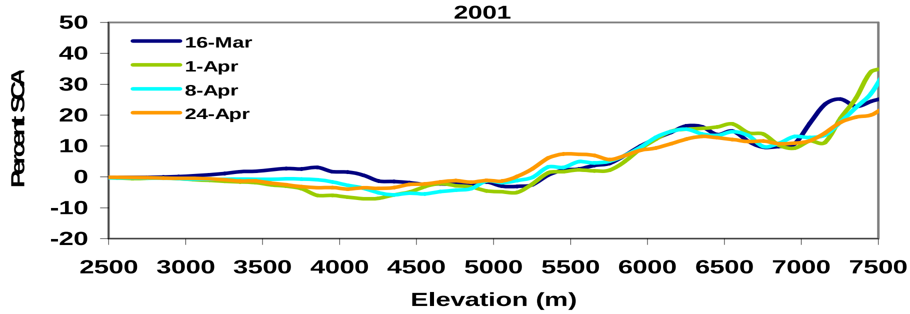

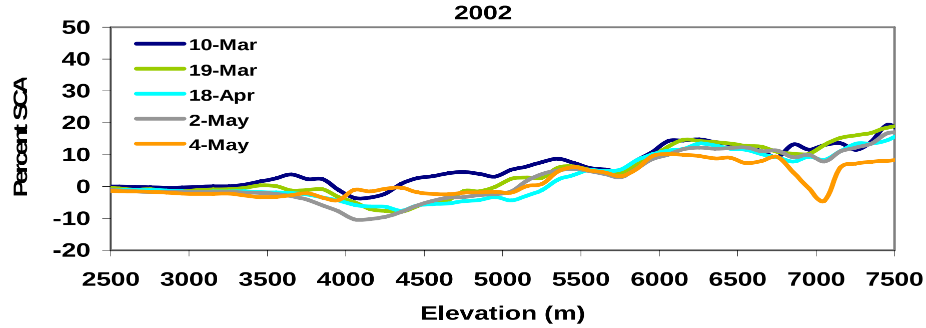

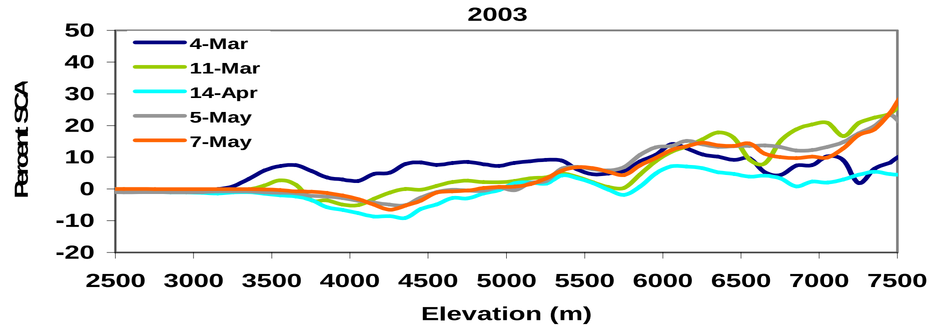

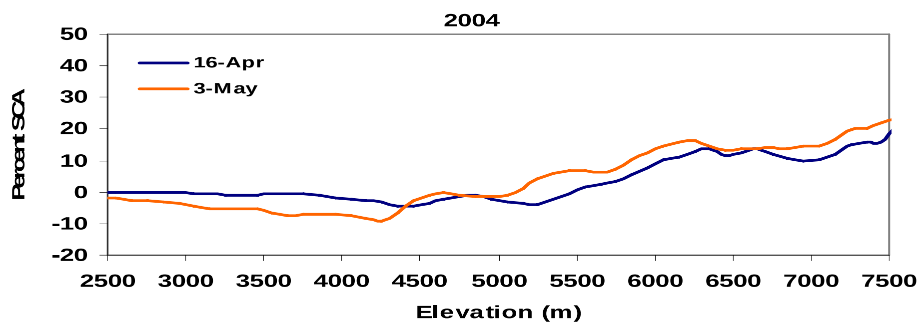

Annapurna study region

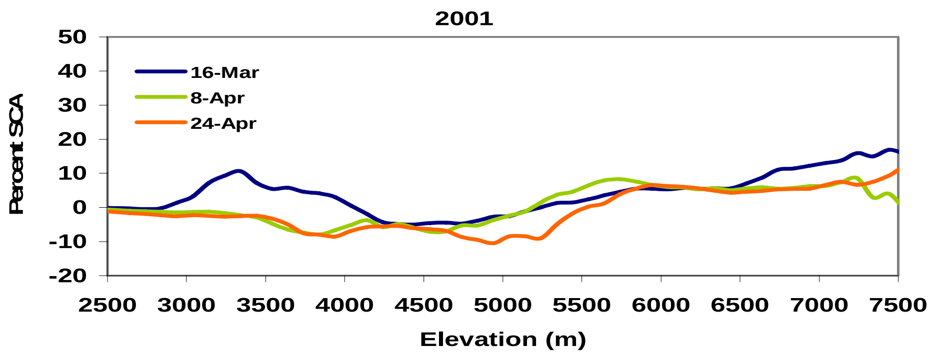

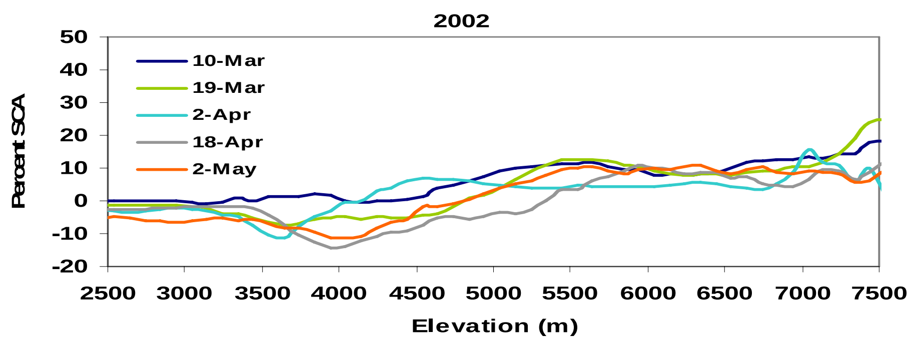

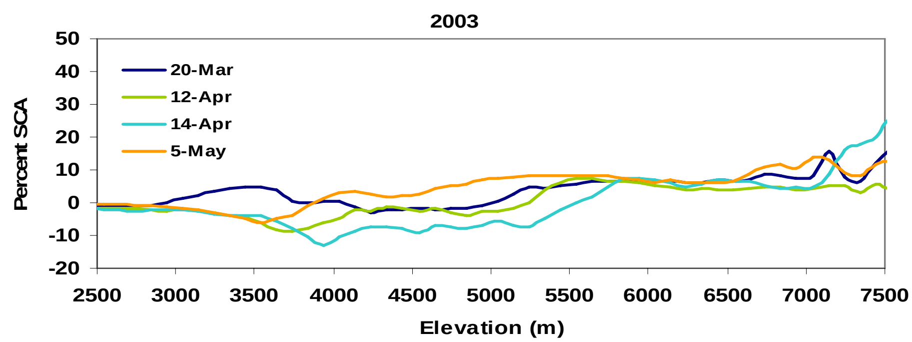

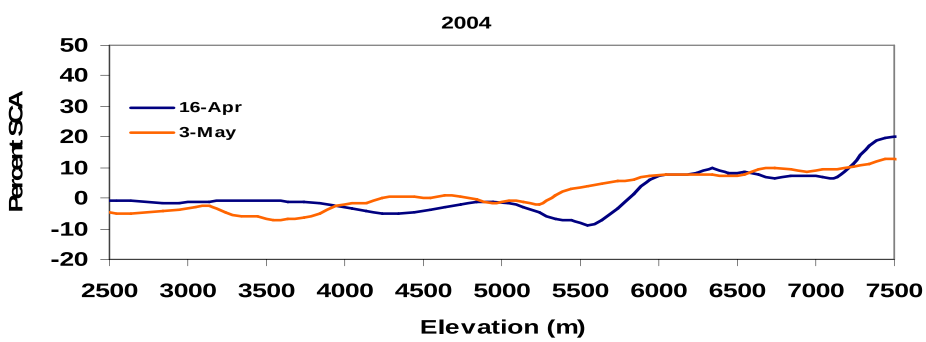

APPENDIX C: Polar plots of percent SCA plotted against Aspect of the Everest study region and the Annapurna study region.

Everest study region (2001)

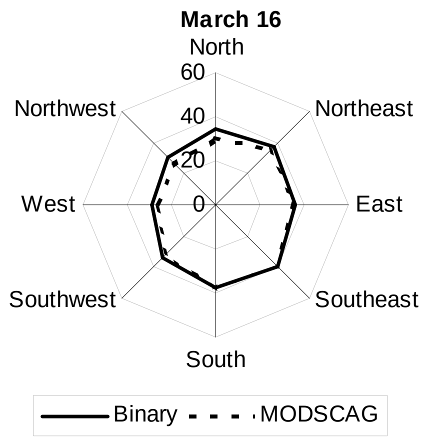

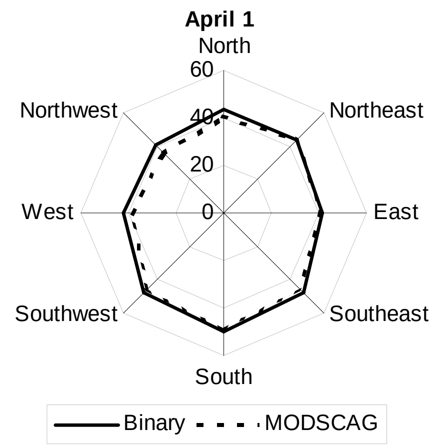

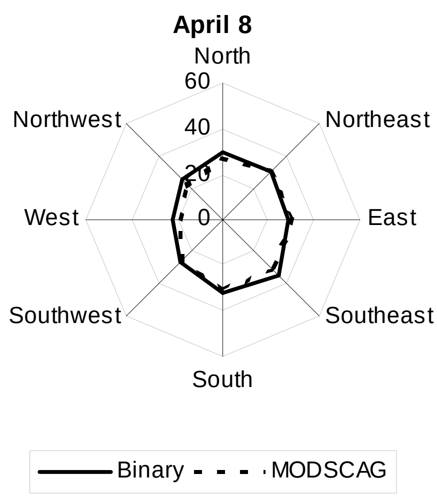

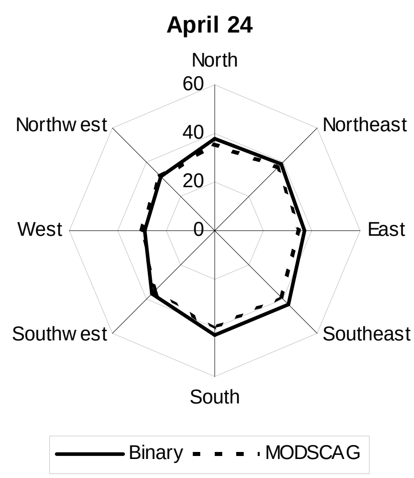

Everest study region (2002)

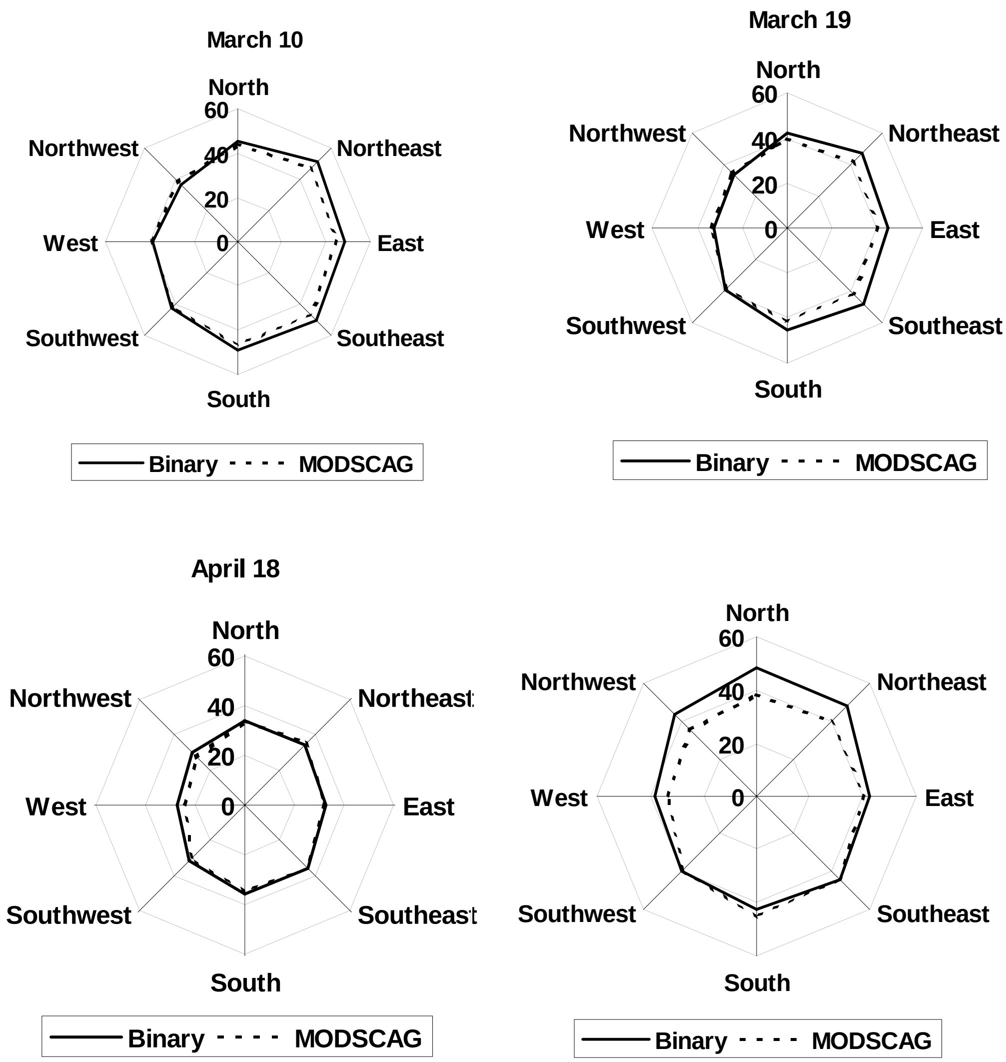

Everest study region (2003)

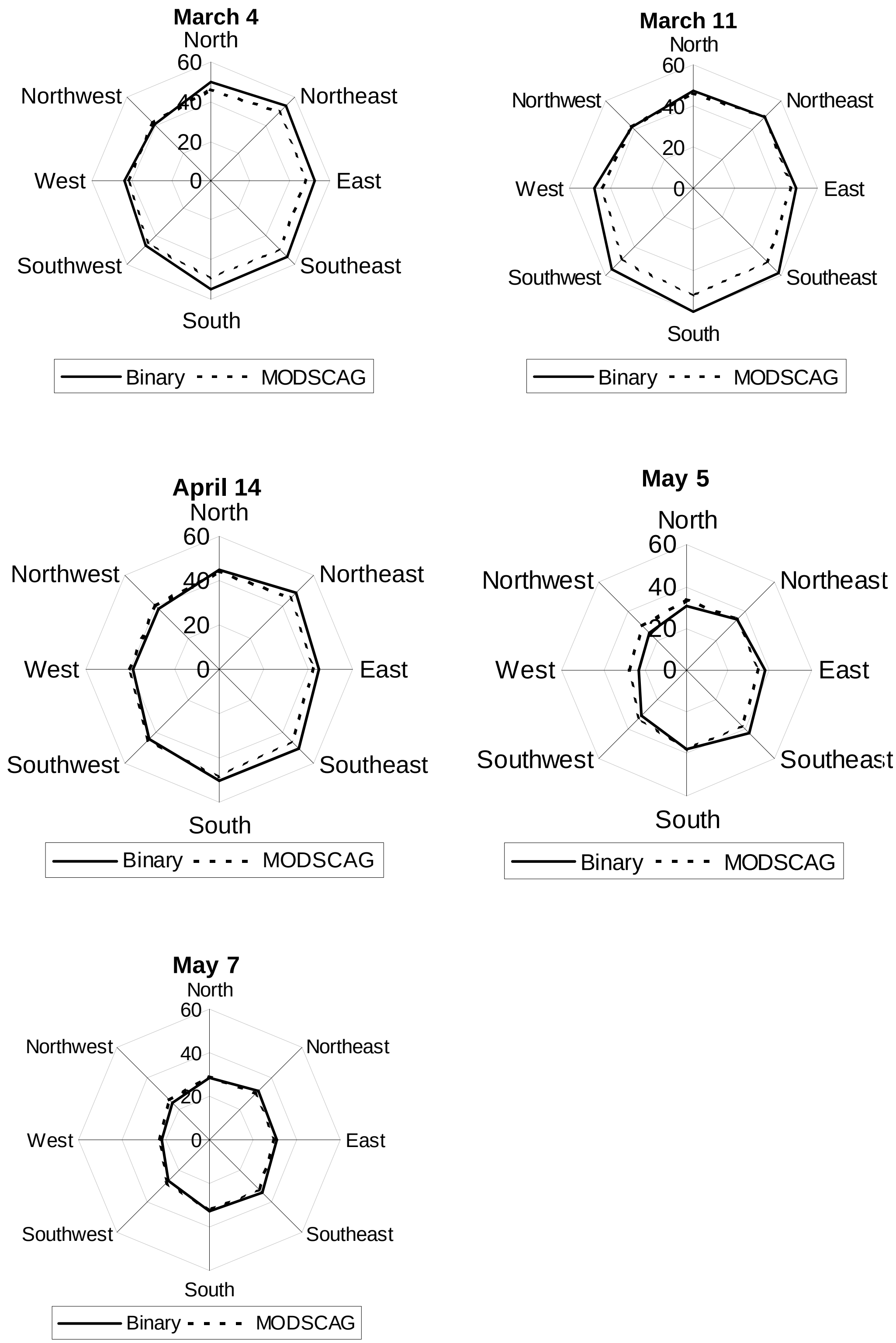

Everest study region (2004)

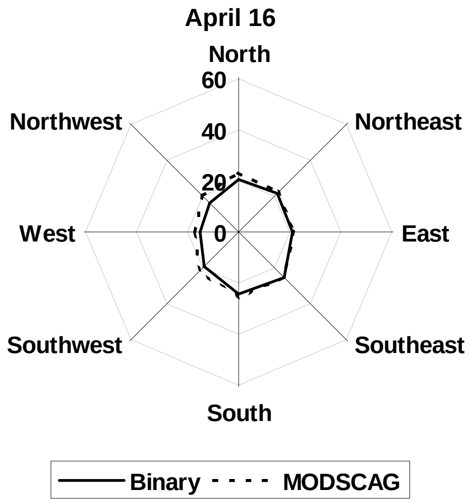

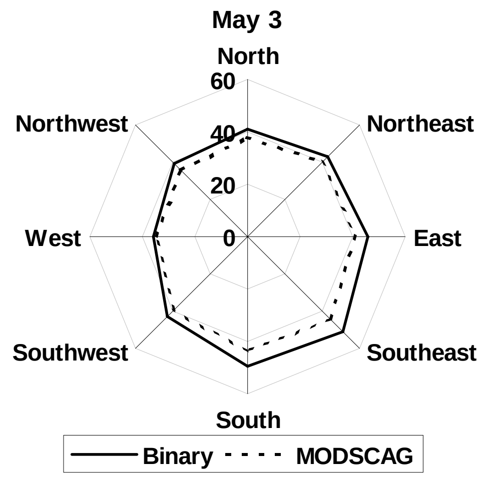

Annapurna study region (2001)

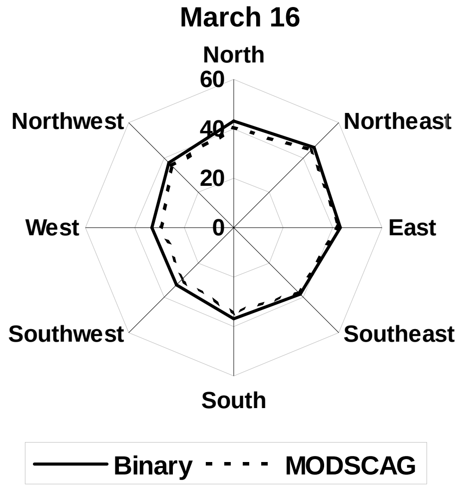

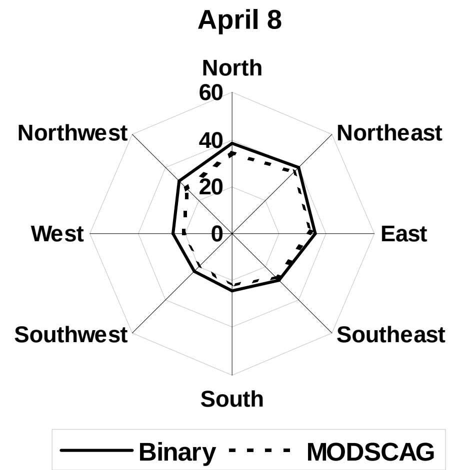

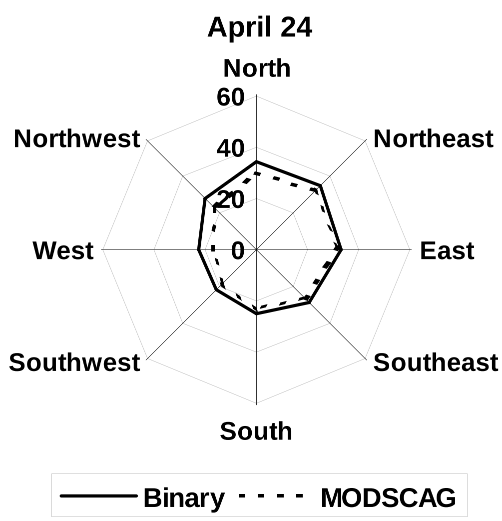

Annapurna study region (2002)

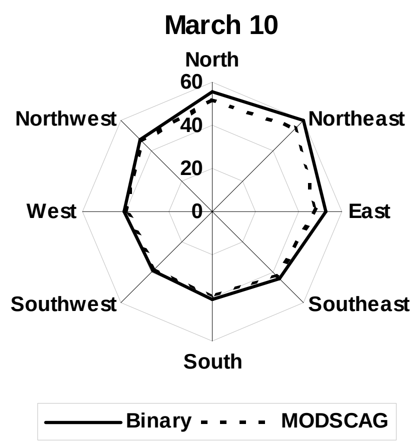

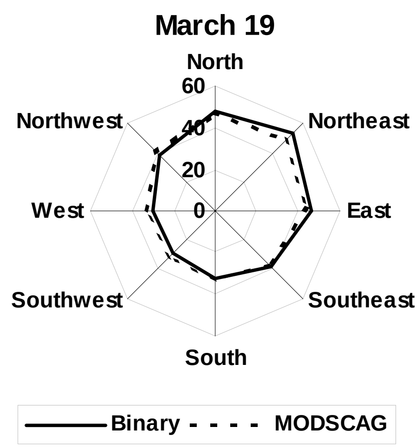

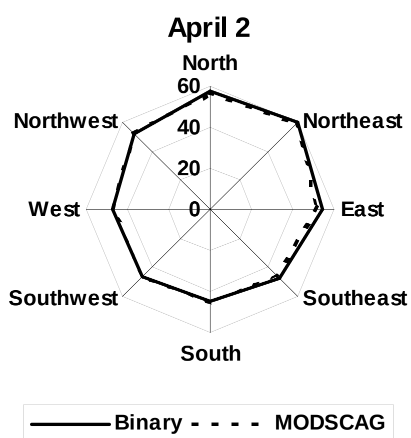

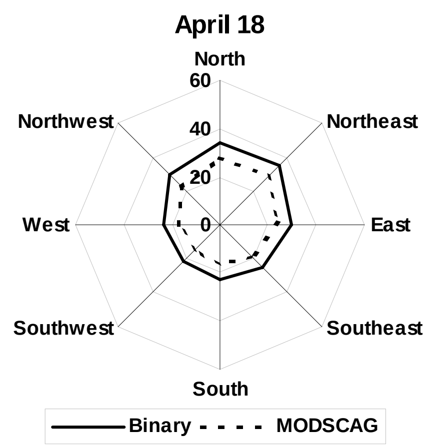

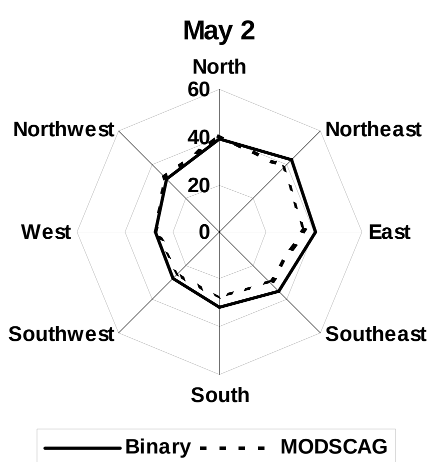

Annapurna study region (2003)

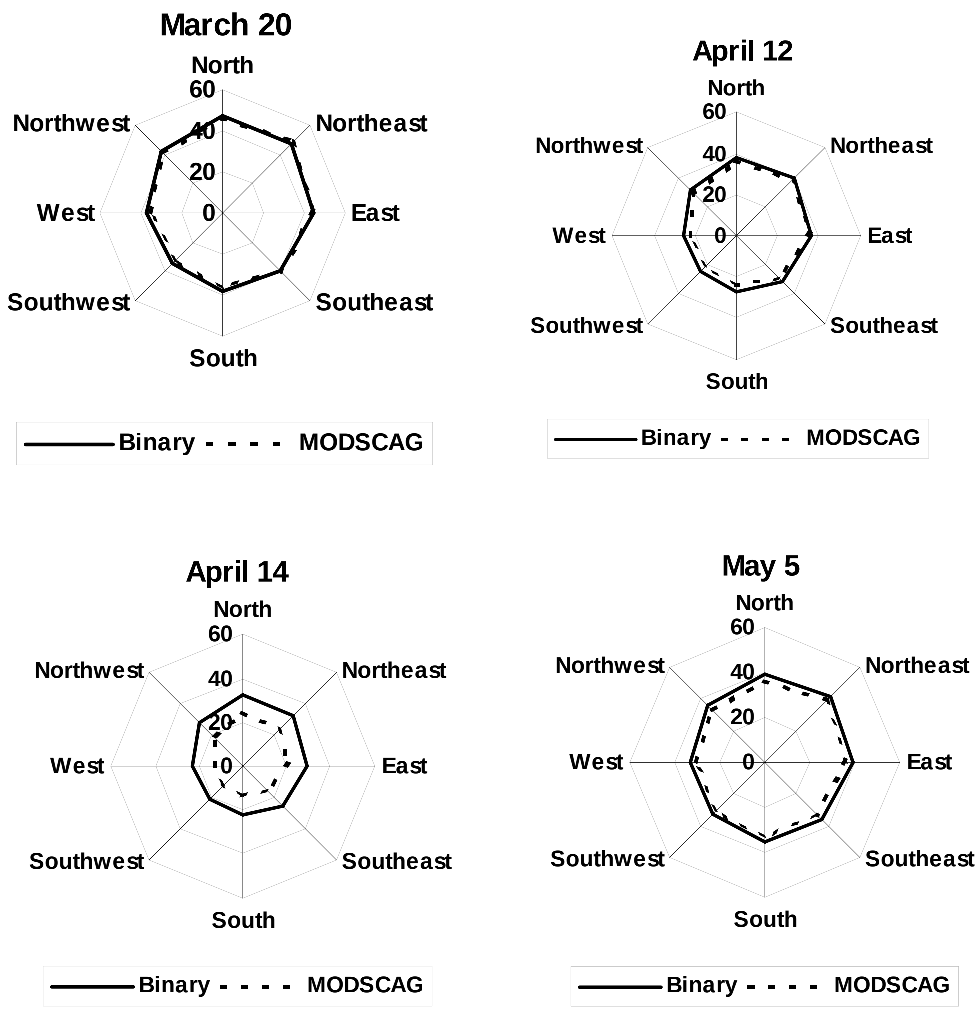

Annapurna study region (2004)

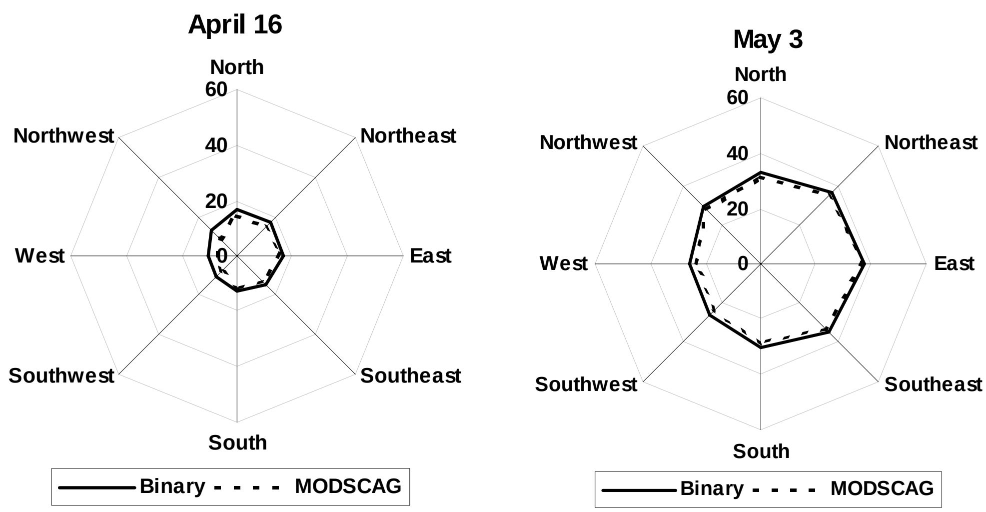

APPENDIX D: Time sequence maps of the Everest study region and the Annapurna study region for the year 2001, 2002, 2003, and 2004.

Everest 2001

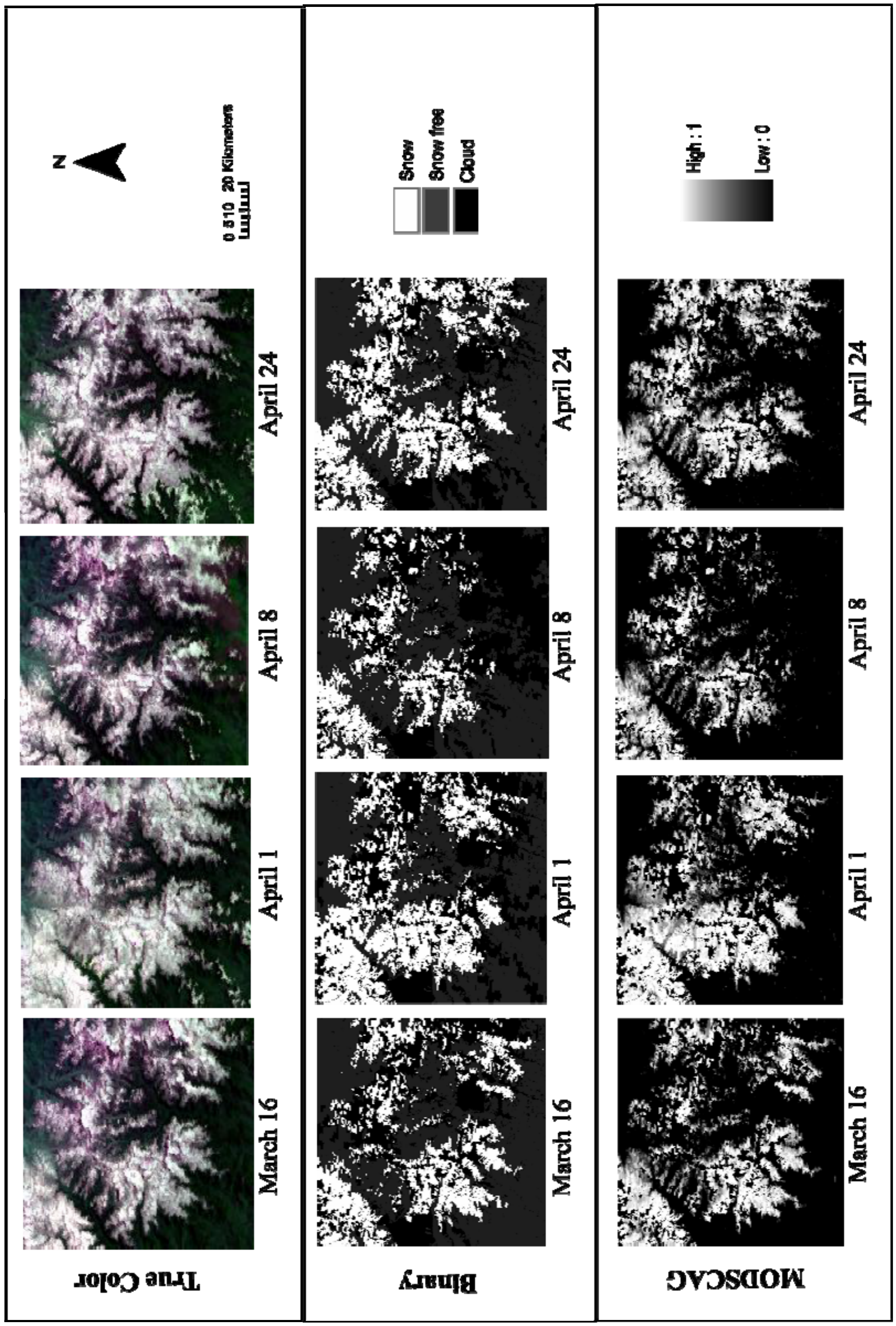

Everest 2002

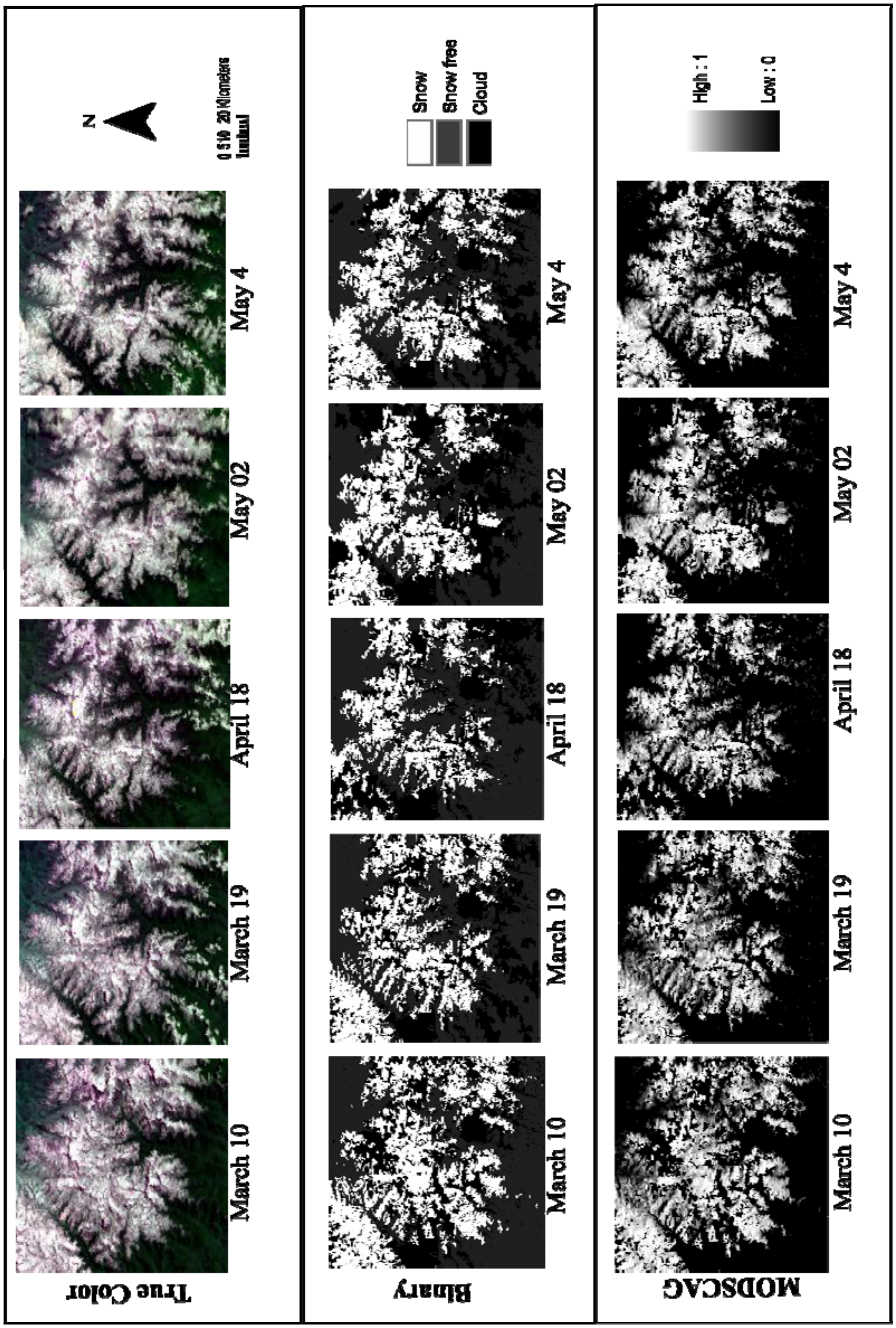

Everest 2003

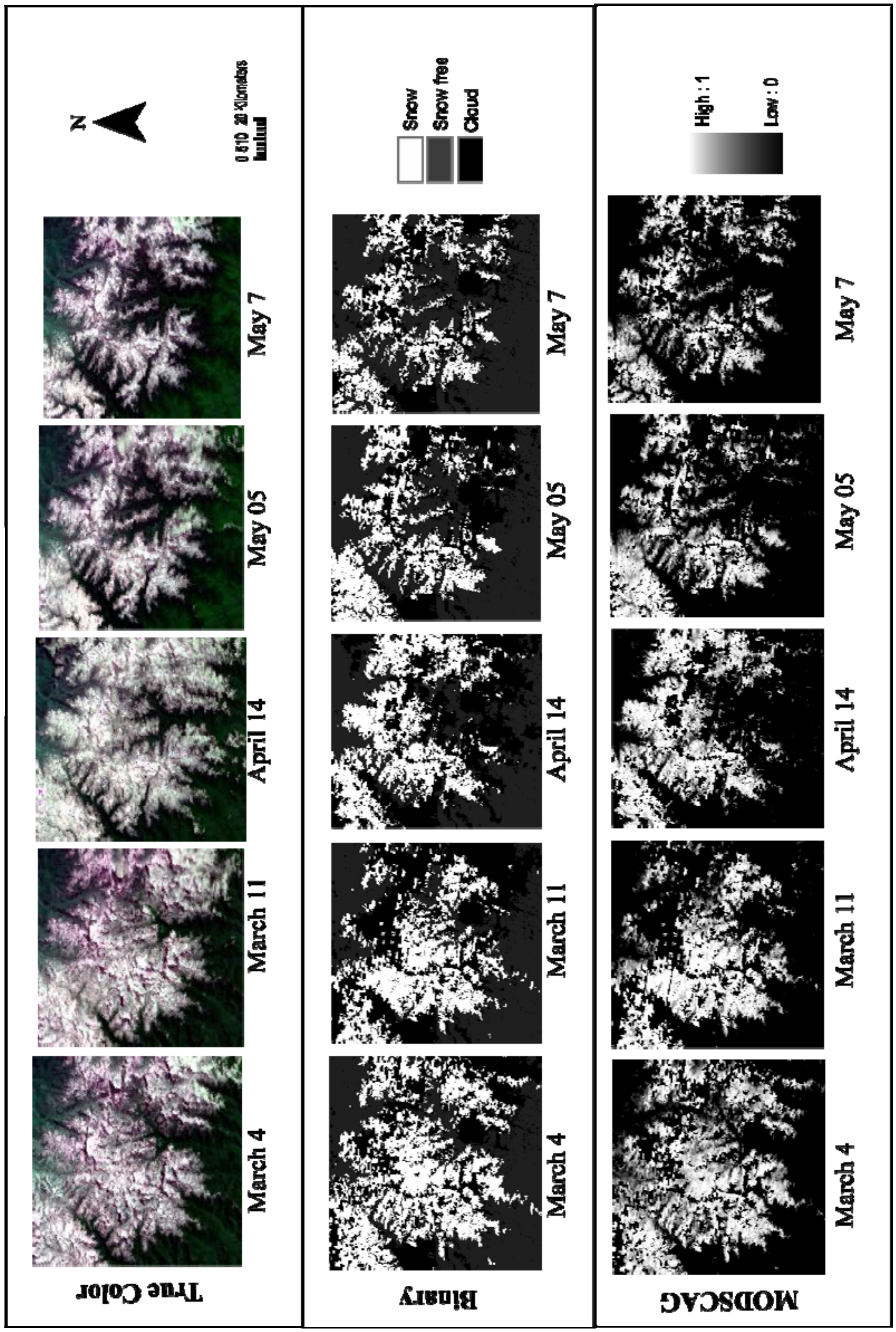

Everest 2004

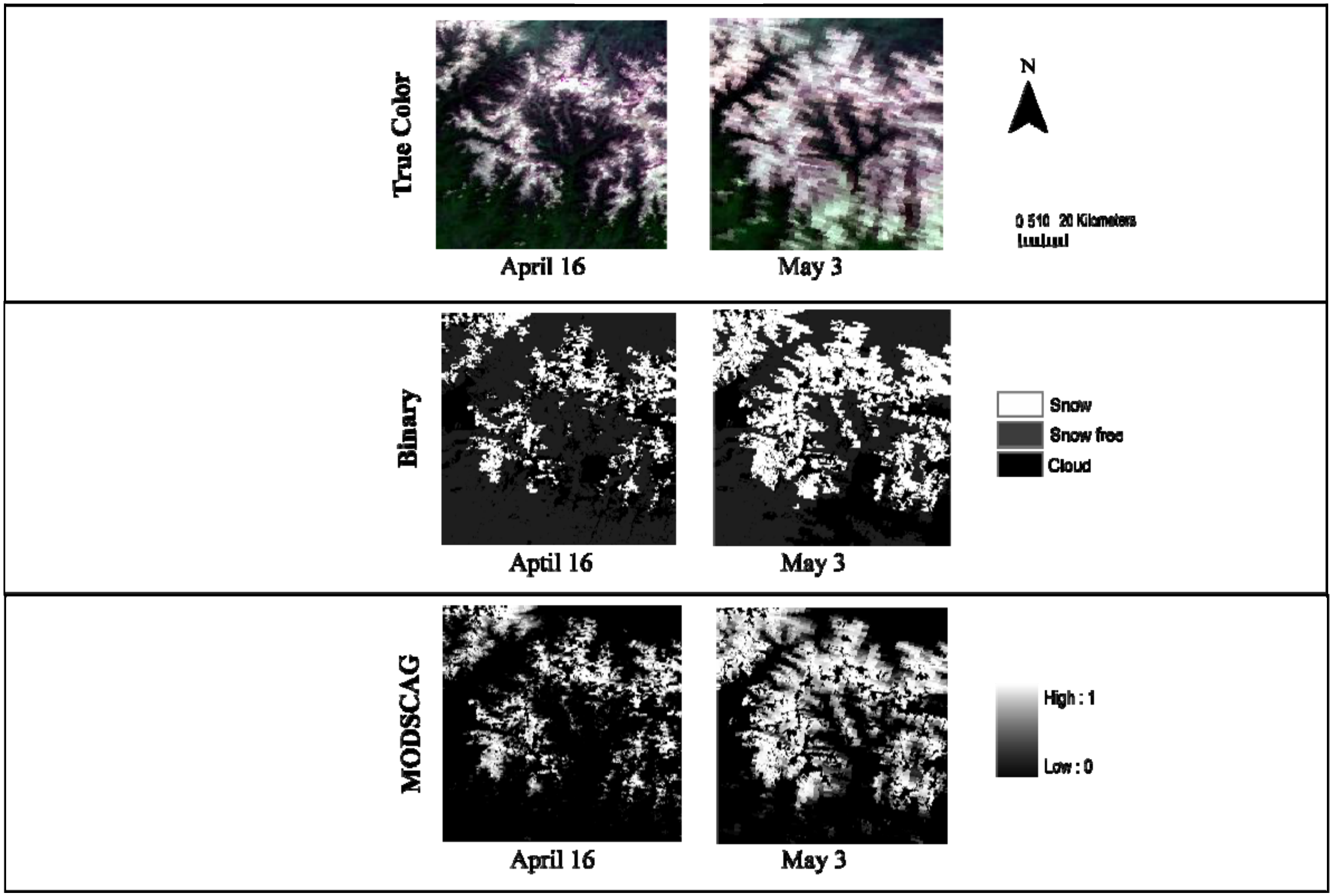

Annapurna 2001

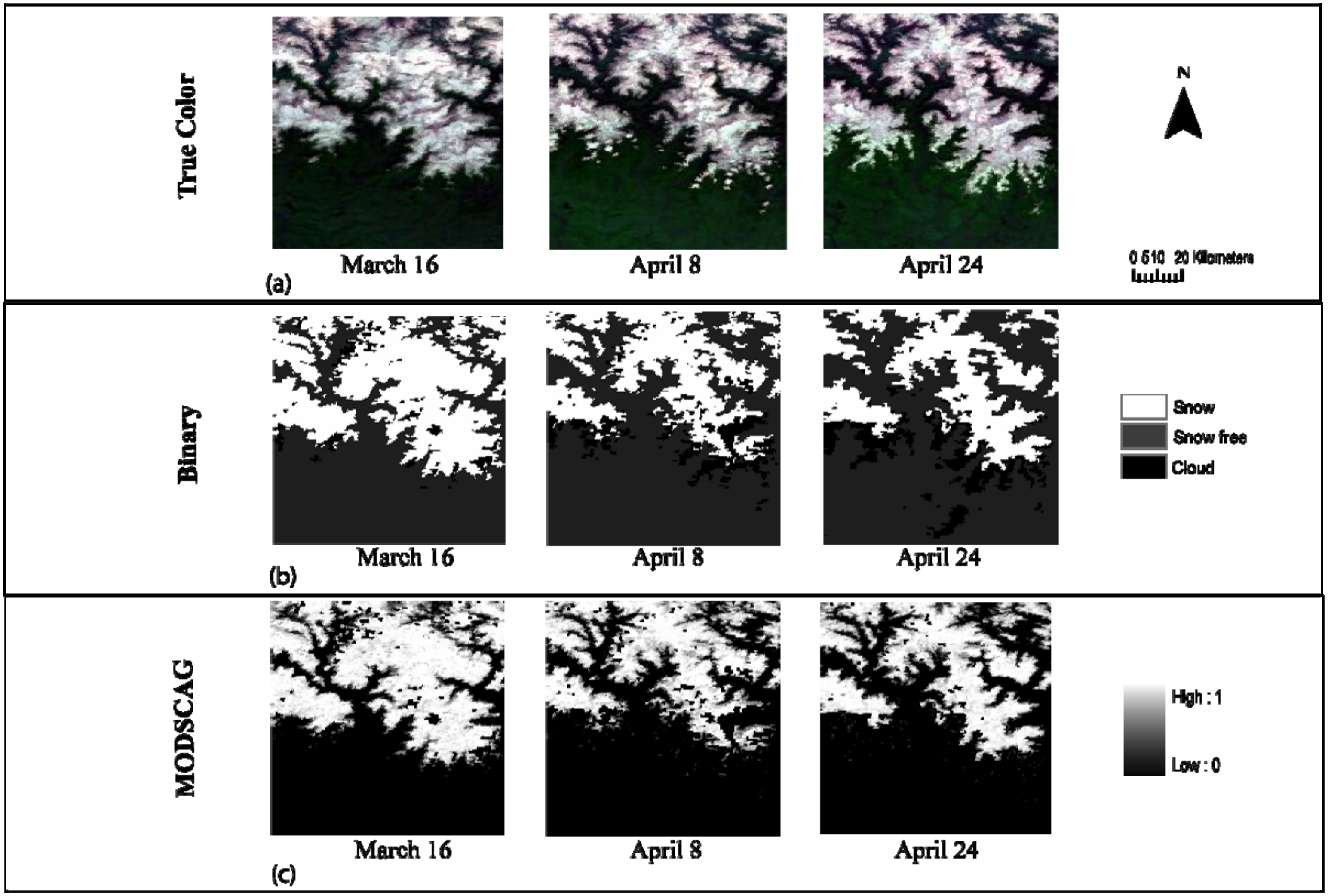

Annapurna 2002

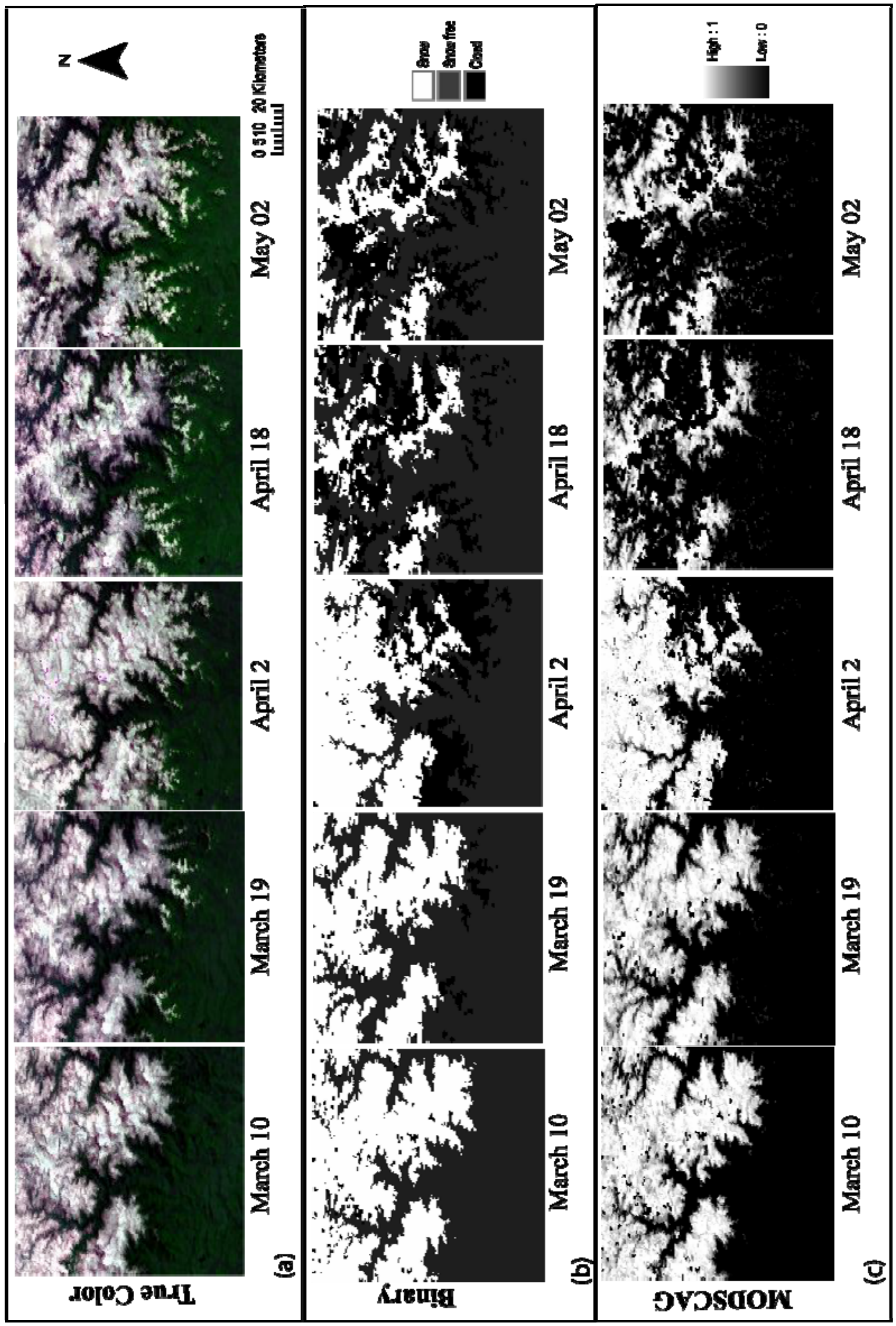

Annapurna 2003

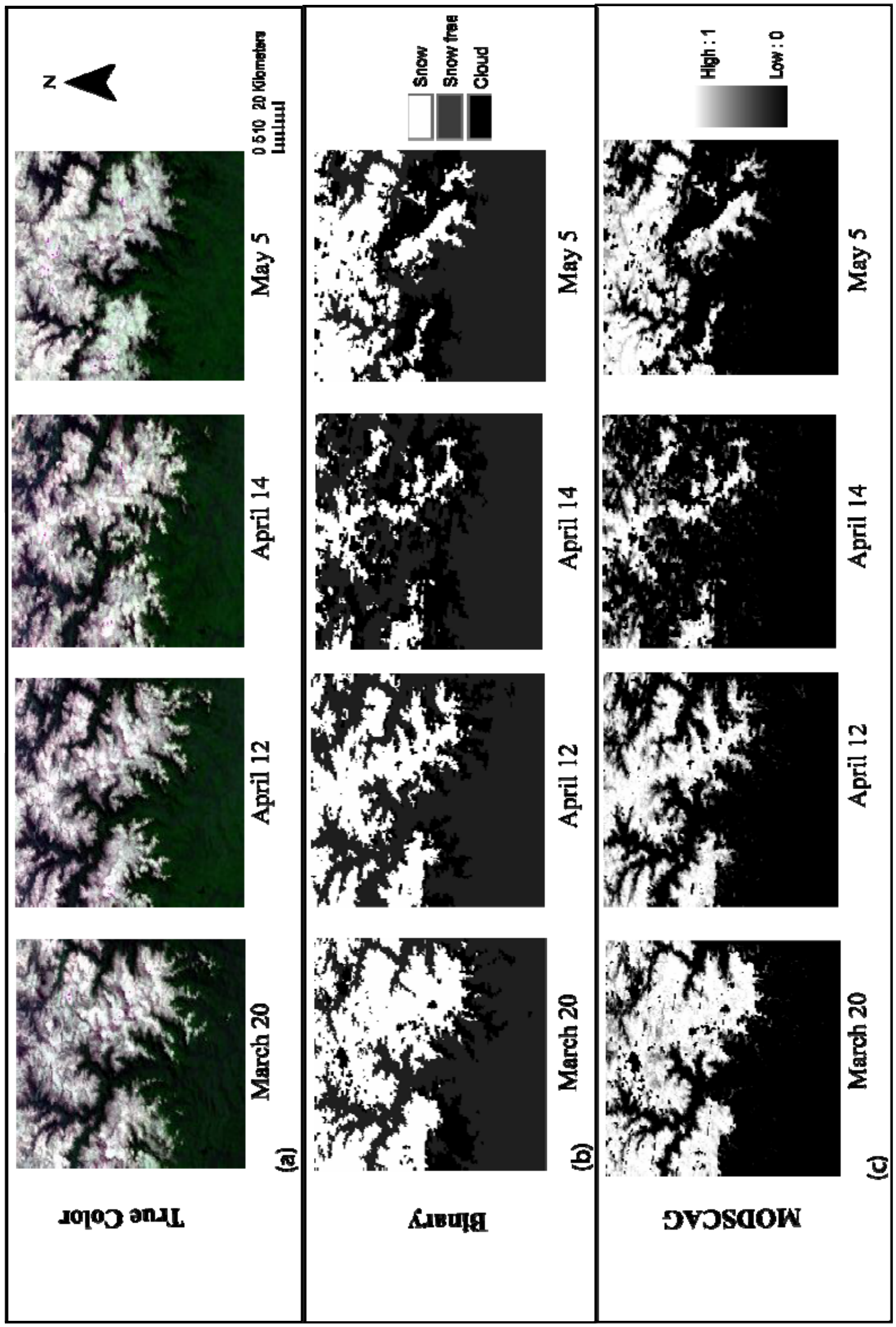

Annapurna 2004